INSTALLATION AND VALIDATION OF AN AIRBORNE DATA ACQUISITION SYSTEM ABOARD A CESSNA 310H FOR USE AS A FLYING LABORATORY

William Thomas Broadhurst

NAVAL POSTGRADUATE SCHOOL
Monterey, California

THESIS

INSTALLATION AND VALIDATION OF AN
AIRBORNE DATA ACQUISITION SYSTEM ABOARD
A CESSNA 310H FOR USE AS A FLYING LABORATORY

by

William Thomas Broadhurst

Thesis Advisor: D. M. Layton

March 1974

Approved for public release; distribution unlimited.

Installation and Validation of an Airborne Data Acquisition System Aboard a Cessna 310H for Use as a Flying Laboratory

by

William Thomas Broadhurst
Lieutenant, United States Navy
B.S., United States Naval Academy, 1967

Submitted in partial fulfillment of the
requirements for the degree of

MASTER OF SCIENCE IN AERONAUTICAL ENGINEERING

from the

NAVAL POSTGRADUATE SCHOOL
March 1974

ABSTRACT

Installation and evaluation of a proposed airborne data acquisition system was accomplished for use aboard the Aeronautical Engineering Department's Cessna 310H. This flying laboratory was obtained for use with the two-course series in flight evaluation techniques to enable students to employ actual flight test methods and to gain an insight into the problems and limitations of flight testing. Static and dynamic analyses were performed on the aircraft's pitot-static boom, and a method was found to dampen vibration of the boom in flight. System calibration procedures were formulated, and the system was tested throughout the flight envelope of the aircraft. The system was found to provide satisfactory data for classroom work and will certainly improve as additional sensors are added.

TABLE OF CONTENTS

ACKNOWLEDGEMENT

The author wishes to thank Associate Professor Donald M. Layton for his guidance and support as thesis advisor and Professor L. V. Schmidt for his continuing interest and assistance throughout the range of this thesis project. In addition the author would like to thank all of the Aeronautics Department technicians who aided in the completion of this project. Special thanks go to Mr. Burtis H. Funk who installed the data acquisition system in N164X.

I. INTRODUCTION

The Flight Mechanics Curriculum of the Naval Postgraduate School's Aeronautics Department includes a two-course series in flight evaluation techniques. The first of these courses introduces methods used in evaluating performance characteristics of aircraft, while the second course investigates stability and control evaluation. In order to make this classroom work more meaningful, it is highly desirable to have access to an aircraft which can function as a flying laboratory. In addition to enabling students to put flight evaluation theory into action, working with an actual aircraft serves to demonstrate problems and limitations of flight testing. The object of this program is not to produce test pilots or flight test engineers, but rather to give aeronautical engineering students a feel for the capabilities of flight test work.

The requirements of such a flying laboratory include the following:

1) An aircraft and data acquisition system that are reliable and relatively inexpensive to operate.
2) A data acquisition system that is not too elaborate - one that is simple and easy to operate. A minimum amount of time should be required in teaching students how to operate the system.
3) A system that actively involves students in the test procedures. One of the main benefits of a flight lab

is that the student can experience what is occurring during a given test. The more actively he is involved in the test, the more aware he will be of what is happening.

4) A system that requires little data reduction. Student time can be utilized more effectively in qualitatively analyzing the flight data.

Until January of 1972, aircraft assigned to the Naval Auxiliary Landing Field were available for use in demonstrating flight test methods. When Combat Readiness Training was discontinued, and the Navy removed all its aircraft from Monterey, it became necessary to seek an aircraft from another source.

Accordingly, a Cessna 310H was leased from a civilian owner through funding provided by Naval Air Systems Command. Because the aircraft is used solely by a government agency, it is defined by Federal Aviation Regulations as a public aircraft. This means that the aircraft is not bound by FAA regulations and that the operating activity is responsible for the safe operation and maintenance of the aircraft. The Aeronautics Department, however, maintains the aircraft in accordance with the requirements for an aircraft certified under a standard air-worthiness certificate, and all applicable inspections and documentation are accomplished as necessary even though not required by FAA. The aircraft is operated in accordance with the Naval Postgraduate School Air Operations Manual, Chapters IV-VII of OPNAVINST 3710.7,

and Federal Aviation Regulations, and where a conflict exists, the most stringent requirements are followed.

A well-structured organization has been formed by the Curricular Office and Department of Aeronautics faculty to oversee operation of the aircraft. This organization provides flight check-out for students who fly the aircraft, and also ensures that the aircraft is properly maintained and operated in a safe and efficient manner. During lab exercises the aircraft is piloted by students who are enrolled in the flight evaluation course; this serves a dual purpose, increasing the utilization of the aircraft by allowing an additional student to participate in each flight, and also allowing the students controlling the aircraft to gain an even greater insight into flight test work.

Installation and check-out of a previously designed data acquisition system was accomplished in the fall of 1973. An initial flight evaluation was conducted in January of 1974, and the system was immediately put into use as a flying laboratory.

II. DATA ACQUISITION SYSTEM

A. AIRCRAFT DESCRIPTION

A photograph of the Naval Postgraduate School's Cessna 310H, N164X, is shown in Figure 1. The aircraft is a low-wing, twin-engine monoplane built by Cessna Aircraft Company in 1963. It is powered by two Continental I0-470-D reciprocating engines with a rated output of 260 horsepower at 2625 RPM. Each engine is equipped with a two-bladed, constant speed, full feathering propeller. The aircraft has tricycle type landing gear which are fully retractable. Maximum gross takeoff weight is 5100 pounds including a passenger/cargo load capacity of approximately 1000 pounds.

The aircraft's primary flight control surfaces consist of conventional rudder, ailerons, and elevator. These surfaces are mechanically linked to a yoke and rudder pedals at each of the two front seats. Three-axis trim capability is provided by trim tabs located on the rudder, right elevator, and left aileron. These tabs are mechanically controlled by trim wheels located on the engine control pedestal. The left (pilot's) instrument panel contains flight and navigation instruments while the right (co-pilot's) panel contains engine instruments. Engine and propeller controls are located on the engine control pedestal, between the pilot and co-pilot.

Aircraft electrical power is supplied by a 28-volt, negative ground, direct current system and is powered by a

50-ampere engine-driven generator on each engine. Two 12-volt batteries are connected in series to provide a standby 24-volt power source when the generators are inoperative. All of the electrical systems in the aircraft are protected by "push-to-reset" type circuit breakers located on the left forward cabin wall. Additional protection is provided to certain circuits by the use of fuses.

The Cessna 310H is designed to accommodate a maximum of six passenger seats. The Postgraduate School's aircraft is configured to carry four people- the pilot, plus three other students. This arrangement allows room for the installation of the data acquisition system and also compensates for the weight of the system.

The flight envelope of the 310 is large enough to enable investigation of many facets of both performance and stability and control. The maximum speed of the aircraft is 254 MPH, with a stall speed of 75 MPH when landing gear and flaps are down. The load factor operating range is from +3.8 g to -2.0 g. With oxygen, the 310 is capable of operating to a maximum altitude of 20,000 feet. The aircraft's two engines provide a means of studying the effects of asymmetric power. The main fuel supply is located in the wing tip tanks, and this presents an available means for examining the effects of asymmetrical loading. In general, the aircraft seems well suited for use as a flight laboratory.

Several previous flight evaluations have been conducted on the Cessna 310. Reference 7 contains a study of the

handling qualities and stability and control characteristics of seven general-aviation aircraft, including the 310. Reference 8 reports the results of full-scale wind tunnel tests of the 310. It contains extensive information on static lateral and longitudinal stability and control characteristics of the airplane. These two reports provide excellent background and comparison material for conducting flight tests with the Naval Postgraduate School's aircraft.

B. OBJECTIVE

The objective of instrumenting the aircraft was to provide an airborne data acquisition system capable of furnishing performance and stability and control data to each of the three passenger seats in the aircraft. Parameters to be measured by the data acquisition system include:

1. Control Force
    a. elevator
    b. aileron
    c. rudder
2. Control Position
    a. elevator
    b. aileron
    c. rudder
3. Angle of Attack
4. Sideslip Angle
5. Normal Acceleration
6. Airspeed
7. Altitude

In addition, engine parameters can be obtained directly from existing aircraft instrumentation.

C. SYSTEM DESIGN

A data acquisition system for the Cessna 310H was previously designed as a thesis project. Reference 5 contains a complete description of the system design and the philosophy that went into its creation. A brief account of the main components of the system design is given below:

1. Measurement of Control Forces

Strain gages arranged into Wheatstone bridge circuits provide an efficient means of measuring applied forces. Accordingly, strain gage bridges were incorporated into the cockpit flight controls to measure elevator, aileron, and rudder forces.

a. Aileron and Elevator Forces

Blueprints for a specially designed control wheel were obtained from Cessna Aircraft Company. This wheel was fabricated by the Aeronautics Department machine shop and installed in the aircraft in place of the existing co-pilot wheel. This new control wheel is essentially two cantilever beams extending from the center control column. These cantilever beams have a rectangular cross section with four type C-9-171 strain gages on each face. The strain gages on each face are wired to form a 350-ohm Wheatstone bridge. The wheel is mounted so that elevator forces and aileron forces are measured independently.

Signal conditioning for the instrumented control wheel is provided by Grant model DCA8-3 operational amplifiers. One amplifier is used with the elevator force system and another is used with the aileron force system. Twenty-eight volt aircraft power is supplied to each amplifier and, in turn, the amplifier provides a five-volt excitation to the appropriate bridge circuits on the control wheel. Output voltage from the bridge circuits is then passed back to the operational amplifier for signal amplification.

b. Rudder Force

Each of the copilot's rudder pedals is equipped with a special force transducer manufactured by Radiation Incorporated. These transducers consist of strain gages arranged in 350-ohm Wheatstone bridges to register the force applied to each rudder pedal. Each pedal transducer is powered by 5 volts from a Grant operational amplifier. The output voltage from each transducer is fed back into its operational amplifier for amplification. The signals from both amplifiers are then added using an electrical algebraic summer. This summer reverses the sign of the signal from the right rudder pedal before combining it with the signal from the left rudder pedal. The signal which comes out of the summer is the differential of the signal from the two rudder pedals and thus represents the differential force that is produced when the pilot uses both feet on the rudder pedals.

2. Measurement of Control Surface Positions

Each of the primary flight control surfaces of the Cessna 310H is mechanically linked to the cockpit controls via wire cables and bell-crank assemblies. Since any angular movement of a control surface is accompanied by a corresponding move in the mechanical linkage, determination of control surface position can be accomplished by measurement of the linkage displacement from some reference point.

In order to measure this control linkage displacement, three linear displacement transducers were obtained from Space Age Control, Incorporated. Each transducer is essentially a 2000-ohm rotary-arm potentiometer with a spring-tensioned spool enclosed inside a drum on the side of the potentiometer. A flexible six-inch wire cable is wrapped around the spool and extends through an opening in the drum. As this wire is pulled out of the drum, the spool turns and the rotary arm turns with it. Likewise, when the wire is released, the spring tension on the spool causes the spool to rewind, and the rotating arm turns in the opposite direction. This action causes the potentiometer resistance to vary from zero to 2000 ohms. When the wire from the potentiometer is connected to a control cable, movement of a control surface causes a change in potentiometer resistance which can be easily measured and translated into measurement of the control surface displacement.

3. Accelerometer

A Statham model ASTC-8.0-350 accelerometer is used to measure the aircraft's normal acceleration. This is an unbonded strain gage type accelerometer which electrically measures g-loading normal to the aircraft's longitudinal axis. The accelerometer is powered by 5VDC from a Grant operational amplifier, and its output signal is amplified by the op amp.

4. Pitot-Static System

In addition to the original pitot-static system installed in N164X, three additional systems were installed to enable investigation of the effects of placement of the pitot-static ports. A 90-inch boom is attached to the left wing tip of the aircraft. This boom extends into the free airstream ahead of the aircraft. A pitot-static tube in the nose of this boom allows measurement of the static and dynamic pressures outside the pressure disturbance caused by the aircraft. An additional pitot-static tube is located under each wing at wing station 161. Plastic tubing from each dynamic and static source is routed through the wings and into the cabin area. Any pitot-static system may be selected for use at any of the three student consoles. No change was made to the original pitot-static system, and it is connected solely to the pilot's flight instruments.

5. Yaw and Pitch Sensor (YAPS)

The boom described in the above paragraph also contains a YAPS head for measuring angle of attack and sideslip

angle. This YAPS head is located on the forward part of the boom and consists of two identical light-weight aluminum vanes. These vanes are mounted perpendicular to each other with the angle of attack vane free to rotate in the vertical plane, and the sideslip vane free to rotate in the horizontal plane. The shaft of each vane is connected to a 5K ohm rotary potentiometer inside the boom. Deflection of the vane causes a corresponding change in the resistance of the potentiometer and enables measurement of the angular deflection of the vane.

6. Junction Box

The central feature of the data acquisition system is the junction box. This J-box serves as a collection point for the inputs from all of the system's electrical sensors. The J-box also houses balance potentiometers for the three flight control surface position transducers and the two transducers located in the YAPS head of the pitot-static boom. These balance pots allow voltage nulling for any desired zero settings of the sensor potentiometers.

The J-box is divided into an input side and an output side. The input side consists of 15 pairs of jack plugs mounted on top of the junction box. Each pair of plugs includes a red plug and black plug. The signal from each of the five sensor potentiometers, the output of the rudder force summer, and the outputs from the elevator force, aileron force, and accelerometer operational amplifiers are wired into these input plugs. The high side of each signal

is fed into the red plug, and the low side is fed into the black plug. Only nine of the 15 pairs of plugs on the input side are used in the present system design. The remaining six sets of plugs were included to accommodate future expansion of the data acquisition system.

The output side of the junction box consists of five pairs of red and black plugs. These plugs are wired directly into the student consoles located at each of the three passenger seats. Any five of the nine available electrical sensors can be patched into the student consoles by linking the input plugs for each of the chosen parameters to a pair of output plugs. Thus, there is a capability of channeling five different signals into the student consoles. The number of output signals passed to the student consoles was based on the determination that a maximum of five electrically measured parameters would be required for any given flight test.

7. Data Presentation

Data presentation is accomplished by an instrument console at each passenger seat. Each console has an airspeed indicator, an altimeter, and a small digital voltmeter. The voltmeter is a DATEL model DM1000 with a display range of ±1.999 volts. A selector switch below each voltmeter allows a choice of any one of the five available parameters. Data from the electrical transducers are presented as an easy-to-read digital voltage, and data reduction consists of simply entering a calibration curve with this voltage to obtain

the actual parameter value. In addition, aircraft engine performance parameters can be easily obtained from the co-pilot's instrument panel.

III. PITOT-STATIC BOOM ANALYSIS

A. BOOM DESCRIPTION

The remote-sensing pitot-static system is installed on the left wing tip of the aircraft as shown in Figures 2 and 3. The system consists of a 90-inch boom protruding into the free air stream ahead of the aircraft, with a YAPS head and pitot-static tube mounted on the tip of this boom. The boom itself is constructed of 1.875-inch diameter seamless 2014T6 aluminum tubing with .136-inch wall thickness. It is secured to the wing by a bracket mounted to the forward wing spar and another bracket mounted to the rear wing spar. The boom is also constrained by a clamp which extends out from the forward bulkhead of the left wing tip fuel tank. Wiring for the YAPS head and tubing for the pitot-static system run down the center of the boom, through the left wing, and into the aircraft cabin.

Cessna Aircraft Company used a similar pitot-static boom when validating the standard 310 pitot-static system. However, no documentation could be obtained to prove that a structural analysis had been done on this boom design. If one examines the flight envelope of the 310H (Figure 4), it is seen that the aircraft is subjected to a fairly wide range of conditions. The 310H has a maximum speed of 254 MPH and normal acceleration ("g") limits of -2g to +3.8g. Since the pitot-static boom was to be a semi-permanent installation on

N164X, it was decided that a complete analysis of the boom system was necessary to ensure safety of flight.

The aerodynamic loading on the boom is a result of the crossflow component of the velocity of the aircraft. Figure 5 is a diagram showing how crossflow velocity is determined. The greatest crossflow due to angle of attack should occur when the aircraft is operating at sea level with maximum gross weight loading and in the clean configuration. Inasmuch as the crossflow velocity is a function of both the angle of attack and the velocity of the aircraft, the extreme points of the V-n diagram (points A, B, and C in Figure 4) were examined to determine the greatest possible crossflow velocity.

Point A

$W = 5100$ lb $\qquad \delta_e = 0$

$V = 254$ mph $\qquad n = 3.8$

$S = 179$ ft^2

$$C_L = \frac{2nW}{\rho V^2 S} = .656$$

The full scale wind tunnel curves for the Cessna 310 [Ref. 8] shows that the above C_L corresponds to an aircraft angle of attack of 6°. Since the boom is at an angle of incidence of -.5°, the actual angle of attack of the boom is 5.5°. This produces a velocity across the boom of:

$$v_{crossflow} = V \cdot \sin \alpha_{boom} = 35.7 \text{fps}$$

The crossflow velocities for points B and C were found in a similar manner:

Point B	Point C
V = 167 mph	V = 86 mph
n = 3.8	n = 1.0
C_L = 1.52	C_L = 1.52
$v_{crossflow}$ = 73.7fps	$v_{crossflow}$ = 37.9fps

Thus, it appears that the greatest crossflow velocity due to angle of attack occurs at point B on the V-n diagram. The Reynolds number for the boom at this point was found to be approximately 6×10^4. Since point B should represent the flight conditions at which the boom would experience its largest aerodynamic loading, a static and dynamic analysis was made using these conditions.

B. THEORETICAL BOOM MODEL

Before attempting a structural analysis of the pitot-static boom, it was first necessary to create a theoretical model of the boom with which to work. As the boom is rigidly fixed to the wing, it was decided to treat the portion of the boom forward of the front wing spar as a cantilever beam. The boom support which is mounted to the tip tank is flexible and bends as the boom moves. Therefore, it was modeled as a spring support. The forward part of the boom contains the YAPS instrumentation, and is much more densely packed than the rest of the boom, so it was modeled as a concentrated

mass on the tip of the boom. The resulting theoretical model is shown in Figure 6.

C. STATIC ANALYSIS

The boom is essentially a circular cylinder and as such, its drag coefficient can be determined from a plot of drag coefficient versus Reynolds number such as shown by Schlichting [Ref. 9]. In a previous section it was shown that the maximum crossflow across the boom corresponded to a Reynolds number of approximately 6×10^4. At this Reynolds number a circular cylinder should have a C_D of approximately 1.2.

In normal flight, the vertical aerodynamic loading on the boom will act in the opposite sense from the loading caused by the weight of the boom. The loading on the boom in the horizontal plane is due to aerodynamic forces alone; no weight component is involved. In order to simplify calculations and to maintain a safety factor, the weight of the boom was neglected throughout the static analysis.

The static analysis was broken down into a superposition of a cantilever beam with a uniform loading (due to aerodynamic drag) plus a cantilever beam with a point load (due to reaction of the spring support). (See Figure 7). For a uniform load on a cantilever beam, the deflection can be expressed as:

$$v_1(x) = -\frac{1}{24}\frac{\omega}{EI}(x^4 - 4\ell^3 x + 3\ell^4)$$

For a point load on a cantilever beam, the deflection is expressed as:

$$\nu_2(x) = -\frac{1}{3}\frac{fx^3}{EI} = -\frac{1}{3}\frac{k\cdot\nu(x)}{EI}$$

Since the deflection of the beam is simply the sum of these two expressions, the deflection at point "a" can be found.

$$\nu(a) = \nu_1(a) + \nu_2(a) = -\frac{\omega}{24EI}\left[\frac{a^4 - 4\ell^3 a + 3\ell^4}{1 + \frac{k\cdot a^3}{3EI}}\right]$$

Using the following properties of the actual boom, the deflection at point "a" was determined.

$E = 10.8\times10^6$ psi

$I = 0.28258$ in.^{4}

$a = 33.25$ in.

$L = 67.94$ in.

$w = q\cdot C_D\cdot D = 0.101 \frac{lb}{in}$

$k_{vertical} = 657.5 \frac{lb}{in}$

$k_{lateral} = 331.5 \frac{lb}{in}$

(See Appendix A for development of spring constants.)

For a vertical loading, the deflection at point "a" was found to be:

$$\nu(a)_{vertical} = 0.00889 \frac{in.}{lb/in.}$$

This results in a spring reaction of

$$f_{vertical} = k_{vertical}\cdot\nu(a)_{vertical} = 5.84 \text{ lb}$$

Likewise, the deflection and spring reaction were found for a lateral loading:

$$\nu(a)_{lateral} = 0.01382 \frac{in.}{lb/in.}$$

$$f_{lateral} = k_{lateral}\cdot\nu(a)_{lateral} = 4.58 \text{ lb}$$

Once the spring reaction forces had been determined, shear and moment diagrams were constructed as shown in Figure 8. Stress along the boom was determined using the expression $\sigma = \frac{MY}{I}$. The maximum stress resulting from aerodynamic loading was found to be 268 psi and occurred at the fixed end of the boom. Tubing of 2014T6 aluminum has an ultimate strength of 62,000 psi and can easily handle the static loading caused by aerodynamic forces.

D. DYNAMIC ANALYSIS

When a circular cylinder is placed normal to an airstream, the wake of the cylinder tends to shed from alternating sides of the rear of the cylinder. The fluctuating wake creates unsteady aerodynamic forces on the cylinder, and if the cylinder were free to move, these unsteady forces would cause the cylinder to oscillate. The frequency (f) at which the cylinder oscillates is a function of the diameter of the cylinder (D), the velocity of the airstream (V), and the Reynolds number of the flow across the cylinder. This relationship can be expressed as $S = \frac{fD}{V}$, where S represents a dimensionless frequency known as the Strouhal number. Strouhal number is solely a function of Reynolds number and body cross-sectional shape and maintains a constant value of approximately 0.21 [Ref. 9] over the range of Reynolds numbers encountered for a circular cross-section of the pitot-static boom. Knowing the Strouhal number and the diameter of the boom, the frequency of oscillation may be determined

for any crossflow velocity. Referring again to the V-n diagram of Figure 4, the following frequencies were calculated:

$$f_A = 48 \text{ hertz}$$

$$f_B = 99 \text{ hertz}$$

$$f_C = 51 \text{ hertz}$$

$$f_D = 17 \text{ hertz}$$

$$f_E = 9 \text{ hertz}$$

An initial experimental investigation was performed on the installed boom to identify its dynamic structural characteristics. A Statham unbonded strain gage accelerometer was strapped to the tip of the boom. This accelerometer was hooked through appropriate signal conditioning and amplification and into an oscillograph. The boom was given a sharp rap, and a time history of the boom vibration was obtained. From this plot a fundamental resonance frequency of approximately 6.5 hertz was found for a vertical input, and a resonance frequency of approximately 10.5 hertz resulted from a horizontal input. The plot also enabled determination of a damping ratio (ζ) of about 0.005 for the boom system. Using the relationship $G = \frac{1}{2\zeta}$, the dynamic gain of the boom could be estimated to be approximately 100.

The next step in the dynamic analysis was to calculate theoretical values for the first and second resonant frequencies of the boom system. These calculations were necessary to provide a cross check for the first resonant frequency found experimentally and to furnish a reliable estimate for the second resonant frequency. In order to obtain reasonably

accurate values for the first two modes, the first four modes were considered. Modal expansion was accomplished using the Rayleigh-Ritz energy method. A candidate admissible function of

$$\phi_n = 1-\cos\left\{\frac{(2n-1)\pi}{2}\cdot\frac{X}{L}\right\};\ n = 1,2,3,4$$

was selected and calculations were performed as outlined by Tong on page 286 of Ref. 11.

.The potential energy of the boom system was determined as the sum of the potential energy due to beam stiffness plus the potential energy due to the spring support of the boom. The kinetic energy of the system was determined as the sum of the inertia effects of the distributed mass of the boom plus the inertia effects of the concentrated mass at the boom tip. The Naval Postgraduate School's IBM 360 computer was utilized to obtain modal frequencies and mode shapes for four different boom configurations. These four configurations included:

1. Boom with no concentrated tip mass and no spring support
2. Boom with tip mass but no spring support
3. Boom with tip mass and vertical spring support
4. Boom with tip mass and horizontal spring support

The computer program that was employed, plus the mode shapes and modal frequencies for each of the four cases are shown in Appendix B and Figure 9. The first two resonant frequencies

for each case are tabulated below for comparison:

Case	f_1(hertz)	f_2(hertz)
1	14.6	92
2	7.5	69
3	11.8	85.5
4	10.3	78

As would be expected, the concentrated end mass had the effect of lowering the resonant frequencies, while the spring support caused an increase in the resonant frequencies. The fundamental resonant frequency for case 4 showed reasonable agreement with the corresponding frequency found by measurement. The first frequency for case 3 differed significantly from the measured value. This difference was due primarily to the coupling experienced between the boom and the wing torsion mode of the aircraft when the case 4 measurement was conducted.

The following structural frequencies were obtained from the Cessna Aircraft Company for the Cessna 310H:

Tip Tanks	Bending	Torsion	
		1st	2nd
Full	2.9 Hz	8.1 Hz	10.8 Hz
Empty	6.4 Hz	11.0 Hz	20.0 Hz

There were three problem areas pointed out by this dynamic analysis. The first resonance frequency of the boom system was found to be in the same range as the structural frequencies of the aircraft's wing. Secondly, the vibrations caused by the unsteady aerodynamic forces on the boom

span the frequency range containing the first and second resonance frequencies of the boom, and the second resonance frequency of the boom is relatively close to the aerodynamic frequency produced by the maximum cross-flow velocity across the boom. When the boom resonance gain of 100 is applied to the maximum static stress, the maximum dynamic stress is found to be about 26,800 psi. For an ultimate boom strength of 62,000 psi, the resulting margin of safety was found to be 1.3. In view of the rough approximations and methods used in determining this margin of safety, it was considered to be much too low. In order to increase the safety margin and to avoid the possibility of wing flutter caused by vibration of the boom, it was decided to seek a means of increasing the damping ratio of the boom. Increased damping would decrease the dynamic gain, decrease dynamic stresses, and reduce the effect of boom-wing coupling.

E. EXPERIMENTAL ATTEMPTS TO INCREASE BOOM DAMPING

Damping is a rather common subject, discussed quite freely in any textbook on mechanical vibration. However, when it becomes necessary to evaluate the damping present in a given physical system, or to increase the damping ratio of a system, it appears much easier and more reliable to resort to empirical methods. Accordingly, it was decided to experimentally seek a practical means of increasing the damping ratio of the aircraft's pitot-static boom.

Since it was not desirable to use the actual pitot-static boom as a vibrational test-bed, a laboratory model of the

boom was created to examine possible methods of obtaining damping. The model chosen was simply an aluminum tube which was mounted as a cantilever beam on the Naval Postgraduate School's 500-pound Ling Temco shaker table. The model was fashioned from two-inch diameter aluminum tubing, 102 inches in length. The tubing was mounted to the shaker table by means of a six-inch clamp which securely held it in place. This arrangement resulted in two identical four-foot cantilever beams extending either side of the clamp and served to reduce any unsymmetrical loading of the shaker table. Dimensions of the model were dictated by a desire to obtain geometric similarity and a system with a resonance frequency close to that of the actual pitot-static boom. The shaker table which was utilized demonstrated questionable accuracy below fifteen hertz, so the model was designed with a first natural frequency of approximately thirty hertz. Although the natural frequencies differed between the boom and the model, they were still in the same immediate frequency range.

Two Endevco piezoelectric accelerometers were calibrated and placed on the model. One accelerometer was mounted at the midpoint of one of the cantilever beams, and the other was mounted on the clamp which held the model to the shaker table. These transducers were used to measure the shaker table acceleration (input) and the resulting response of the model (output). Data acquisition instrumentation included a digital frequency counter, an RMS voltmeter to determine input and output signals, and a dual beam oscilloscope for

signal visualization. A photograph of the shaker table layout is shown in Figure 11. The ratio of the output to the input, or magnification ratio, could then be determined over a suitable frequency range to provide information on the vibration characteristics of the model. From a plot of magnification ratio versus frequency, the resonant frequencies and damping ratios could be determined from the relationship

$$\zeta_n = \frac{\Delta f}{2f_n}, \text{ where}$$

$\Delta f \equiv$ 1/2 power band width

$f_n \equiv$ resonant frequency of the n^{th} mode

$\zeta_n \equiv$ damping ratio of the n^{th} mode

The first and second mode shapes of the basic pipe model were obtained. From these mode shapes the mode frequencies and modal damping could be determined. This information was used as a basis for comparing the relative effects of various attempts to add damping to the system.

Several of the methods employed in the search for a practical damping device are discussed below:

1) The first attempt involved placing a soft wooden dowel inside the entire length of the pipe model. The dowel was fitted snugly into the pipe, and was held in place by set screws. The effect of the dowel was to decrease f_n and increase the magnification ratio, resulting in a damping ratio of approximately fifty percent less than the damping ratio of the basic model.

2) Two small plastic containers were fitted into the last twelve inches of the free ends of the pipe. These containers were filled with water to determine if the sloshing action of the water would create a damping effect. Another test was conducted using a more viscous liquid for comparison. The effect caused by both liquids was similar. The resonance frequency was reduced, and the magnification ratio was reduced, but the overall effect was a lowering of the damping ratio of the system. This was just the opposite of the effect being sought.

3) It was next desired to examine the effects that applying fiberglass to the outside of a beam would have. Lack of facilities ruled out the possibility of applying fiberglass to the pipe model used in previous tests, so it was necessary to use a smaller model for this test. Two identical aluminum bars were obtained, and when mounted on the shaker table each bar formed two symmetrical cantilever beams 12-inches × 1-inch × 3/8-inch. Although there was neither geometric nor resonant similarity between these models and the pitot-static boom, qualitative information could still be obtained. One of the bars was used as a reference, while the other was covered with five layers of fiberglass. The layers were applied alternately in the longitudinal and lateral directions to obtain a total fiberglass cover approximately 1/32-inch thick. Each of these bars was subjected to shaker table tests, and plots of frequency versus magnification ratio were obtained for each bar. Comparison of the

two plots showed that the bar with the fiberglass coating had more than double the damping ratio of the control bar. This seemed to offer a possible solution to damping out the vibrations of the boom, but since a method for applying fiberglass to the actual boom was not readily available, it was decided to search further for an alternative.

4) The Grumman S-2 aircraft has a hollow appendage located on the left horizontal tail. This appendage is partially filled with lead shot and its purpose is to help suppress aerodynamic flutter on the horizontal tail. It appeared that this type of device might provide a suitable method for reducing the vibrational response of the pitot-static boom. Accordingly, a quantity of #9 lead shot was obtained and shaker table tests were conducted using the shot and the pipe model. It became immediately obvious that the shot rattling around in the pipe did have a very noticeable effect on the vibrational characteristics of the model. As can be seen in Figure 11, the shot bouncing around inside the pipe practically destroyed the peaks previously found in the plot of frequency versus magnification ratio. When the pipe was vibrating at frequencies near the model resonance frequencies, the shot could be heard rattling very actively. In addition, the oscilloscope trace for the output signal showed quite a bit of noise when the shot was in motion. Apparently, the irregular bouncing motion of the lead shot against the pipe and against each other tends to dissipate the system's energy at or near the resonance frequencies.

This damping principle is referred to as impact damping and is often used in design of heavy machinery.

A shot package could have the capability of greatly increasing the damping of the boom, but several questions needed to be answered in deciding how to use the shot:

1) Where should the shot be placed?
2) How much shot should be used?
3) What type of container should be used to hold the shot?

The problem of a suitable container for the shot was addressed first. To avoid structural problems and to prevent unwanted aerodynamic effects, it was determined that the shot package should be located inside the boom rather than in an externally-added compartment. There were two constraints on fabricating a shot container. Naturally, it was necessary to allow the shot to vibrate freely within the pipe, yet not allow it to escape. Secondly, provision had to be made to accommodate the wiring and tubing that runs down the center of the actual boom. The setup decided upon was constructed using an 18-inch length of 5/8-inch diameter thin-walled plastic tubing and three two-inch wooden plugs. The tubing was inserted through holes in the center of each wooden plug to form two six-inch compartments as shown in Figure 12. This arrangement allowed the selection of two different locations for the shot, and also allowed the size of the compartment to be varied - all without having to relocate the container assembly within the model. An identical

container set-up was inserted into each end of the pipe model, and as before, symmetry was preserved when conducting vibrational tests using the lead shot.

The next step was to decide what quantity of shot would provide the best damping action for the model. This was accomplished by conducting shaker table tests with varying amounts of shot, but with the shot always in the same location. The first run was conducted using 500 grams of shot, representing about a 50% addition to the weight of the basic model. Following runs were conducted using 250 grams (≈25% of basic model), 125 grams (≈12% of basic model), and 50 grams (≈5% of basic model). Each of these tests was conducted with the shot in a six-inch compartment at the tip of the pipe. Results for the different weights of shot are shown in Figure 13. Surprisingly, varying the amount of shot had little effect on the maximum magnification ratio of the model. However, as the amount of shot was reduced, the frequency range over which the shot was active widened. For all of the various amounts of shot tested, the maximum magnification ratio was approximately four for the first mode, as compared with a maximum ratio of about 21 for the basic pipe without shot. The effect on the second mode was even more dramatic, with a reduction of the ratio from almost 300 down to about five.

To determine what effect position of the shot would have, a series of shaker table tests were carried out utilizing a constant weight of shot and varying the location of the shot

within the model. The sectioned container assembly was mounted at the tip of the model, and 250 grams of shot was placed in the outer six-inch compartment for the first test run. The next run was performed with the shot in the inner compartment. The third run was made with the shot in a six-inch compartment located at the base end of the model, adjacent to the shaker table mount. The results of varying the location of the shot are shown in Figure 14. The maximum magnification ratios for the first two runs were approximately the same, but the outer compartment loading affected a wider frequency range than the inner compartment loading. For the third run, with the shot in the base of the model, the maximum ratio was about seven.

Effect of the size of the shot compartment was considered next. The location and quantity of the shot was maintained constant, and the size (length) of the compartment was varied. Two hundred and fifty grams of shot was placed in the tip of the model, and compartment lengths of three inches, six inches, and ten inches were compared. It was found that increasing the size of the container resulted in a lowering of the maximum magnification ratio. This comparison is shown in Figure 15.

One further test was made to examine the action of the shot inside the model. Since all previous tests had been conducted with the model completely level, it was essential to look at what effects gravity might cause if the model were inclined at some angle such as the boom might experience in

flight. Accordingly, the shaker table was tilted at an angle of twenty degrees to the horizontal, and 250 grams of shot was placed in a compartment at the tip of the model. Figure 16 shows that the frequency response of the tilted model was almost identical to the response of the similarly configured level model. Twenty degrees should be about the maximum combination of angle of attack and pitch angle encountered in flight, so no other angles of tilt were examined.

The vibrational tests performed on the boom model by no means presented a completely optimum solution to the problem of boom vibration. Time restraints prevented a more thorough determination of the best damping procedure, but the work accomplished did present a reasonable answer to the problem at hand. After examining the results of the shaker table tests on the pipe model, it was decided to install a ten-inch compartment containing 600 grams of lead shot (about 15% of cantilevered portion of the boom) as near to the tip of the boom as possible. The compartment was constructed from a twelve-inch length of 5/8-inch diameter thin-walled aluminum tubing with one-inch wooden plugs on either end. The wooden plugs were carefully machined to fit inside the boom, coated with a wood sealer to prevent deterioration of the wood, and bonded to the aluminum tubing with epoxy glue. The compartment was placed inside the boom, loaded with shot, and secured in place with safety-wired set screws.

IV. SYSTEM INSTALLATION AND VALIDATION

A. INSTALLATION

Installation of the data acquisition system was accomplished essentially in accordance with Reference 5, but several changes and additions were necessary in order to make the design functional.

1. Description

a. Transducers

Location of most of the transducers was dictated by the system design. Photographs of the instrumented control wheel and the rudder force transducers are shown in Figures 17 and 18. The rudder pedal transducers may be removed from the aircraft when not required. Total weight change caused by these transducers is three pounds at fuselage station 8.5. Installation of the special control wheel caused negligible weight change from the original control wheel. Mounting of the remote sensing boom was discussed in Section III and is shown in Figure 2.

The ideal location for the accelerometer is at the aircraft's center of gravity. However, there was no available site at or near the c.g. where the accelerometer could be mounted without necessitating an undesirable modification of the aircraft's interior. The transducer was mounted on a five-inch by 1.5-inch aluminum plate and bolted to the floor of the aircraft on the centerline at fuselage

station 67.20. Weight of the accelerometer and plate is about .7 pounds.

In order to minimize the effects of control cable stretch, the rudder and elevator position transducers were located as near to the control surfaces as possible. Both of these transducers were mounted to the aircraft's fuselage structure, and can be reached by removing the tail cone at the rear of the fuselage. The rudder transducer was mounted at station 216.8 (.13 pounds) and the elevator transducer was mounted at station 239.1 (1.0 pounds). With each control surface held in the neutral position, the wire from each potentiometer was extended approximately three inches (of a total six-inch length) and secured to the bell-crank assembly of the appropriate control surface in a non-interfering manner. This allows a maximum control cable travel of three inches in each direction and is more than adequate to accommodate any control deflection that should be experienced.

Space limitations prevented the placement of the aileron position transducer adjacent to an aileron. It was necessary to mount this potentiometer under the cockpit floor, near the point at which the control cable from the right aileron connects with the center aileron bell-crank (station 60.5, .13 pounds). This potentiometer can be reached through a small access panel located just aft of the right front seat, adjacent to the right cabin wall.

b. Junction Box and Signal Conditioning

A 20-inch by 24-inch plate of 1/4-inch thick aluminum was mounted to existing baggage tiedowns in the rear of the aircraft cabin by use of four 1/4-inch - 24 steel bolts at fuselage stations 100.375 and 109.375. The J-box, rudder summer, Grant op amps, and system electrical power supply are all located on this plate. (See Figure 19). The plate serves as a central connection point for all of the data acquisition wiring. Total weight of the plate and its contents is 19 pounds centered at station 104.88.

c. Consoles

One of the instrument consoles is located between the two front seats for use by the copilot (see Figure 20), and the other two consoles are mounted to the rear of the front seats for use by the rear seat passengers (see Figure 21). The front console caused a weight addition of 8.5 pounds at station 45.75 while the rear consoles added 17 pounds at station 54.50.

d. Wiring and Tubing

Electrical wiring between the transducers, junction box, and instrument consoles was accomplished using four-wire shielded 22AWG cable. All cable shields were grounded at the aluminum plate holding the junction box. Cabling is secured to the aircraft cabin floor with plastic clamps, and all electrical leads through aluminum sheeting are protected by rubber grommets. Hook-up of the additional pitot-static systems was accomplished using 1/4-inch O.D.

plastic tubing. It was necessary to pass electrical and pitot-static leads from each wing through the engine nacelles and into the aircraft cabin. These leads were bundled and routed through the nacelle areas using aluminum conduit for heat protection.

2. Power Supply

The electrical power supply for the data acquisition system is 28 VDC which is obtained from the main aircraft electrical power supply. Connection was accomplished by hooking into the existing wiring for the cigarette lighter located at the left rear passenger seat. According to Reference 2, the voltage at this cigarette lighter should be 12 VDC. This 12 VDC is obtained by passing 28 VDC through a dropping resistor. In order to get the necessary 28 volts required by the data acquisition system, the system wiring was connected at a point prior to this dropping resistor.

By linking into existing aircraft wiring it was possible to utilize existing circuit protection. This protection consists of a ten-amp circuit breaker located on the pilot's main circuit breaker panel and a six-amp fuse located under the pilot's instrument console. The circuit breaker is labeled RIGHT LDG LT/REAR CIGAR LIGHTER. The fuse is the top fuse in a bank of three, and it may be seen by looking upward from the pilot's rudder pedals, just below and to the right of the pilot's control column. The electrical load of the entire data acquisition system is approximately three amps.

Power distribution for the data acquisition system is accomplished by use of two bus bars: a +28VDC bus, and a ground bus which is connected to the negative side of the aircraft battery. Power for the force transducers and the Statham accelerometer is obtained directly from these bus bars. Twenty-eight volts is fed into each Grant operational amplifier where it is reduced to a regulated five volts and passed on to the appropriate transducer. Power required for the surface position potentiometers is also five VDC, but since no amplification of the output signal is desired, it was not necessary to use op amps. The 28VDC is reduced to five VDC by passing it through National Semiconductor miniature voltage regulators. Original design called for use of 15VDC with the potentiometers in the YAPS head. However, problems were encountered with the available 15VDC regulators, and it was decided to use 5VDC vice 15VDC with the YAPS transducers. The voltage drop was accomplished identically to the drop for the surface position pots. Each of the five potentiometer sensors has its own dedicated voltage regulator, and these regulators are mounted on top of the J-box. The 5VDC required for each digital voltmeter is obtained by use of a miniature voltage regulator mounted inside each console.

3. Documentation

All alterations and additions made during installation of the data acquisition system were documented using FAA Form 337. Additionally, all work was inspected by an FAA Authorized Inspector.

B. PROBLEM AREAS

Several problems were encountered in implementing the data acquisition system design. The major problem involved possible vibration of the remote sensing pitot-static boom and is discussed at length in Section III. Other problem areas are discussed below.

1. Console Location

The original system design called for the two rear student instrument consoles to be bolted to the back of the two front seats. This arrangement presented a possible danger to the rear seat passengers. If the passengers were thrown forward during an emergency landing, their heads would strike the consoles. Location of the consoles could also present an obstruction to emergency egress from the aircraft. Accordingly, the rear console mountings were modified so that they could be easily removed in flight and the consoles stowed safely away. The consoles were mounted on two metal dowels which fit into holes in the top of the front seats. The consoles are held in place by elastic bungee cords which reach from the bottom of each console to the floor. The consoles can be easily removed by releasing the bungee cords and lifting the consoles upward. The same bungee cords are then used to secure the consoles in an out of the way position under the front seats. (See Figure 21).

2. Potentiometer Circuits

Each of the potentiometer circuits (control surface position indicators and YAPS head) is arranged in a balance

bridge to provide an adjustable zero setting. As a result, the voltage measured by each potentiometer circuit is a differential signal vice a single ended input. It was found that when the output of these potentiometer circuits was measured with a very reliable digital voltmeter, the voltage varied significantly from the signal displayed by the console voltmeters. Reference 4 states that the maximum common mode voltage which can be handled by the Datel voltmeters is ±2 volts. Investigation showed that the common mode voltage of each of the potentiometer circuits exceeded these limits over at least part of their range. This excessive common mode voltage caused the console voltmeters to saturate and display an erroneous output signal.

Since the purpose of the output signal is to provide an indication of control surface or vane position, accuracy of the voltage is not essential. Calibration curves were constructed using the console voltmeters, and while the resulting plots are not linear, they at least provide correct position information.

3. Voltage Regulators

When the National Semiconductor voltage regulators were originally installed, it was found that they heated up excessively when power was applied. Heat sinks were installed in an attempt to reduce the heating, but this was only partially successful. Dropping resistors were incorporated to drop the system's 28VDC down to about 8VDC before feeding it into the voltage regulators. This completely removed any problem of the regulators overheating.

4. Electrical Noise

The signal produced by each of the force transducers is very small. By the time this signal is routed to its operational amplifier in the rear of the aircraft cabin, the signal-to-noise ratio is fairly low. The resulting amplified signal is quite noisy. Some noise is present in the potentiometer circuits, but the signal-to-noise ratio is much higher, and the signal is considerably cleaner.

5. Voltmeter Sampling Rate

The Datel digital voltmeter is designed to sample an analog signal at the rate of 200 times per second. Because of the extreme sensitivity of each output signal plus the high noise level present in some signals, this high sampling rate caused such a rapidly changing signal display that it was impossible to read it. The sampling rate was halved by use of a capacitor (see Ref. 4), but this rate was still much too rapid.

A workable solution was reached by installing an "inhibit switch". This switch was placed on the copilot's console, and when it is actuated it samples and holds whatever signal is currently displayed on each of the three consoles. When the switch is returned to its OFF position, the normal sampling rate resumes until the switch is again actuated.

C. INITIAL CALIBRATION

Once the system installation had been completed, an initial calibration of the entire data acquisition system was

necessary. Calibration procedures were formulated for future use and are included in Appendix C.

1. Voltmeters

Voltmeter calibration was accomplished in accordance with the manufacturer's instructions. (See Ref. 4). Three adjustments were required during this calibration - balance control adjustment, zero control adjustment, and full scale control adjustment. These adjustments were made using three control screws located on the voltmeter face as shown in Figure 22. An additional test was conducted to ensure that all display segments of the voltmeter were working properly. Step by step calibration procedures are listed in Appendix C.

2. Position Indicators

Calibration of the three flight control position indicators was relatively simple. Each flight control surface was held in the neutral position, and the voltage output from each position signal was nulled using the appropriate balance potentiometer located on the J-box. A clinometer was placed on the right aileron, and the aileron was varied through the range ±20 degrees in five-degree increments. A plot of aileron position versus output voltage was obtained and is shown in Figure 23. Elevator position calibration was accomplished in the same manner. The elevator was varied through the range +25 degrees to -15 degrees and the resulting plot is shown in Figure 24. Although the hinge line of the rudder is not vertically oriented, Ref. 2 states that

rudder deflection should be measured in the waterline reference plane. Accordingly, a protractor was constructed to fit between the rudder and fuselage with its center at the rudder hinge line. The rudder was varied through the range ±25 degrees, and the resulting plot of voltage versus rudder position is shown in Figure 25.

3. YAPS Head

Calibration of the angle of attack and sideslip vanes was similar to the calibration of the surface position indicators discussed above. A protractor was placed at the base of the AOA vane, with its center coinciding with the center of the vane shaft. The vane was varied through the range ±35 degrees from the neutral point, and voltage versus AOA was recorded (Figure 26). The same procedures were followed for the sideslip vane, and the calibration curve is shown in Figure 27.

4. Force Indicators

Calibration of the force sensing indicators consisted of adjusting the output signal of each Grant operational amplifier. These amplifiers are capable of producing a five-volt positive signal, but they saturate at approximately .7 volts in the negative sense. When the range of the digital voltmeters is taken into account, an output range of +1.999 volts to -.7 volts can be obtained from these op amps. The GAIN of each amplifier was adjusted to accommodate the maximum possible forces experienced by each control system, while providing maximum amplification of the transducer signal.

a. Elevator

The instrumented control wheel was removed from the aircraft and mounted to a rigid structure. Power supply and wiring identical to that in the aircraft was hooked into the elevator strain gage bridges, and the ELEVATOR FORCE op amp from the aircraft was used to amplify the bridge signal. Known forces were applied to the center of each side of the control wheel in the fore and aft directions by use of a pulley and cable set-up. The GAIN of the op amp was adjusted to obtain an output signal of 15 millivolts per pound. A calibration curve for the elevator force system is shown in Figure 28. After the control wheel and op amp had been replaced in the aircraft, this calibration curve was confirmed by use of a hand-held force gage.

b. Aileron

Calibration of the aileron force system was conducted similarly to the calibration of the elevator force system. Known forces were applied to both sides of the wheel in the vertical direction, and the GAIN of the AILERON FORCE op amp was adjusted to furnish an output signal of approximately 15 millivolts per pound. The elevator force calibration curve is shown in Figure 29. As before, this curve was confirmed by use of a hand-held force gage once the system had been re-installed in the aircraft.

c. Rudder

Calibration of the rudder force system consisted of adjustment of the GAIN of both Grant op amps in the

rudder force system. Because of complexities caused by the rudder summer, it was decided to calibrate each op amp separately. The right rudder force transducer was removed from the rudder pedal and placed on a level area of the cabin floor. Weights were stacked on the transducer, and the RT RUDDER FORCE op amp GAIN was adjusted to obtain a signal output of ten millivolts per pound. The LFT RUDDER FORCE op amp GAIN was adjusted in a similar manner. A rudder force calibration curve is shown in Figure 30. Both op amps were reconnected to the rudder summer, and the calibration curve was confirmed by use of a hand-held force gage.

5. Accelerometer

A complete investigation of the dynamic response of the accelerometer had been conducted previously (see Ref. 5). An abbreviated static calibration of the accelerometer was carried out by means of the turnover method. The sensing axis of the transducer was placed level to the earth's surface, and the ZERO screw of the ACCEL op amp was adjusted to provide a zero signal output for this zero g condition. Next, the accelerometer was rotated until its sensing axis was exactly vertical (+1g), and the GAIN screw was adjusted to provide a signal output of +500 millivolts. The accelerometer was then turned upside down to ensure that the -1g condition produced an output of -500 millivolts. The accelerometer was previously found to have a linear response in the range -2 to +6g, and this encompasses any load factor that N164X might experience in normal flight.

D. FLIGHT EVALUATION

The data acquisition system (minus the pitot-static boom) was tested throughout the flight envelope of N164X. All of the systems appeared to work satisfactorily with one exception. The accelerometer output signal was so noisy in flight that it was practically useless. Use of the inhibit switch was of no assistance with the accelerometer - it only served to sample and hold an erroneous signal.

There were several system-related deficiencies noted, also. With the rudder force transducer blocks installed, the copilot's brakes were almost impossible to use. While this is not a safety hazard, it is a less than optimal condition. Accordingly, the rudder pedal force transducers are installed in the aircraft only on flights where rudder force information is necessary. Another problem area involves the instrumented control wheel. When it is desired to obtain aileron or elevator force measurements, the student occupying the copilot's seat must fly the aircraft. The primary flight instruments are all located on the pilot's side of the aircraft. This, combined with the copilot's unfamiliarity with the aircraft, makes it difficult for him to control the aircraft smoothly. This leads to erratic elevator/aileron force indications. Finally, it is difficult to read the output of the digital voltmeters on each instrument console when the aircraft is operating in bright sunlight.

V. CONCLUSIONS AND RECOMMENDATIONS

The data acquisition system installed in N164X is elementary, but workable. The system has several problems areas which need to be corrected, but it is functional and allows the aircraft to be used as a flying laboratory. Installation of additional sensors will enhance the usefulness of the system. The remote-sensing boom will be installed as soon as FAA approval can be obtained. Three rate gyros and a trailing cone for use as a remote static source are ready for installation when feasible. A suitable alternative for the existing accelerometer should be sought. The inhibit switch which was installed to provide a sample-and-hold capability was merely a stopgap measure. If the signal which is being sampled has a high noise component, then the data obtained are not very reliable. Some means should be sought to either filter out noise before the signal is fed into the digital voltmeter, or to slow the voltmeter sampling rate down to a useable level.

Future plans for the aircraft include a complete revamping of the system signal conditioning. Thought should be given to placing amplification for the force signals as close to the transducers as possible to provide a high signal-to-noise ratio. A voltmeter selector switch with a dedicated position for each individual electrical transducer would be much more convenient than the cumbersome patching system

used in the present system. To overcome the difficulty caused by sunlight shining on the voltmeter face and obscuring the signal, some type of hood or sun shield should be placed around each console voltmeter.

To obtain better results from the control force systems, one of two alternatives should be considered. Either the instrumented control wheel and rudder force transducers should be moved to the pilot's side of the aircraft, or the students who fly as copilot should be given some sort of familiarization training before they attempt to provide control force data.

Work is currently underway on a photo panel for use with the aircraft's data acquisition system. Some type of recording device such as a tape recorder or an oscillograph is needed to help gather dynamic stability and control information. Any future additions or modifications to the data acquisition system must include the student as an integral part of the data-taking process. One of the most attractive features of a flying classroom is the ability to get the student actively involved in flight evaluation.

APPENDIX A

DETERMINATION OF SPRING CONSTANTS FOR THE FORWARD BOOM SUPPORT

In order to model the boom accurately, it was first necessary to determine the spring characteristics of the forward boom support. This support consists of two 2-inch by 1/8-inch straps of sheet aluminum which are welded to a heavy, 3/8-inch circular aluminum collar as shown in Figure 31. When mounted on the aircraft the free ends on the two straps are bolted to the top and bottom of the forward bulkhead of the left tip tank, while the collar fits snugly around the boom.

In order to investigate the spring tendencies of this support, the boom was removed from the support and taken off the aircraft. It was evident that merely applying a force to the support and measuring its deflection would produce meaningless information. The result would be a combined function of the air pressure in the aircraft tires and the twist and bending of the wing, as well as the deflection of the boom support. In order to cancel these unwanted effects, a stiff pipe was mounted in the same position as the boom but extended only up to a position just prior to the support. A Scherr Tumico dial gage was mounted on this pipe so as to measure any vertical deflection between the pipe and the strap. A second dial gage was mounted on the pipe to measure deflection between the pipe and the support in the horizontal

direction. In effect, this pipe created a moving reference point which would indicate only deflections caused by the twisting and bending of the actual boom support and would negate any other deflections. A photograph of this reference set-up is shown in Figure 32.

By use of pulleys and a tripod, the collar of the support was loaded vertically upward in five-pound increments to a maximum load of thirty pounds. Both the vertical and horizontal deflection was recorded at each weight increment, and a graph of force versus deflection was plotted to determine the vertical and horizontal spring constants. This procedure was repeated three additional times with the boom support loaded vertically downward, horizontally inward, and horizontally outward respectively. The spring constants for each load condition were determined from plots of force versus deflection as shown in Figures 33 and 34.

The spring constants were found to be essentially constant for each load configuration over the load range examined. However, the spring constants for the upwardly loaded support were found to be slightly different from those determined by a downward loading. Likewise, the values determined were different when the outwardly loaded case was compared with the inwardly loaded case. These results are reasonable for an irregular shaped spring such as the boom support.

The spring constants found by the above method were a function of the boom support and the wing tip tank on which it is mounted. In order to determine how much of the spring

action is directly attributable to the support alone, a second series of measurements were made with the support mounted to a rigid structure. A full-size wooden mock-up of a cross section of the left wing-tip tank was created. This wooden mock-up provided a means of maintaining the shape and position of the boom support in the laboratory. The support was mounted to the mock-up using the existing screw holes, and this assembly was clamped to a rigid beam. As before, the support was loaded in four different directions, and the spring constants were determined from a plot of force versus deflection. A photograph of the lab set-up is shown in Figure 35, and the force/deflection plots are shown in Figures 36 and 37.

When these spring constants were compared with the values found for the support-tip tank combination, it was determined that a large portion of the spring action in the vertical plane was due to the bending and twisting of the wing tip tank. A smaller, but still significant, part of the spring action in the horizontal plane was also found to be due to the tip tank structure. These results led to the conclusion that even if a completely rigid forward boom support was used, there would still be some spring action resulting from the twisting and bending of the tip tank.

The actual forces which the forward support exerts on the boom in flight are a result of the support-wing tip tank combination, so the spring constants determined by the first method were the values used in all theoretical calculations.

```
C.....................................................................
C..                                                                   ..
C..    VIBRATIONAL ANALYSIS OF THE PITOT-STATIC BOOM                  ..
C..       USING THE RAYLEIGH-RITZ ENERGY METHOD                       ..
C..                                                                   ..
C.....................................................................
C..                                                                   ..
C.. DEFINITION OF TERMS:                                              ..
C..                                                                   ..
C..           INPUT DATA:                                             ..
C..                                                                   ..
C..    BS(I,J) = BEAM STIFFNESS MATRIX                                ..
C..     S(I,J) = SPRING STIFFNESS INFLUENCE MATRIX                    ..
C..    CM(I,J) = BEAM MASS MATRIX                                     ..
C..   CNE(I,J) = CONCENTRATED TIP MASS INFLUENCE MATRIX               ..
C..     SRATIO = SPRING STIFFNESS RATIO, KSP/KB                       ..
C..       CMU  = MASS RATIO, (TIP MASS)/(BEAM MASS)                   ..
C..      CONST = SCALING FACTOR, ML/KB                                ..
C..                                                                   ..
C..           OUTPUT DATA:                                            ..
C..                                                                   ..
C..      EV(I) = EIGENVALUES (OMEGA**2)                               ..
C..    FREQ(I) = NATURAL FREQUENCIES, HZ                              ..
C..     P(I,J) = MODAL MATRIX                                         ..
C..     V(I,K) = MODE SHAPE                                           ..
C..      XL(K) = BEAM STATION, X/L                                    ..
C.....................................................................

      DATA ICASE/1/, CONST/0.48040E-03/,PI/3.14159265/
      DIMENSION BS(4,4),S(4,4),CM(4,4),ONE(4,4),TITLE(9,60)
     1 ,A(4,4),B(4,4),EV(4),FREQ(4),P(4,4),V(4,20),XL(20)

C.. INPUT THE BASIC MATRICES:

  100 READ(5,10)((BS(I,J),J=1,4),I=1,4)
      READ(5,10)(( S(I,J),J=1,4),I=1,4)
      READ(5,10)((CM(I,J),J=1,4),I=1,4)
      WRITE(6,11)
      WRITE(6,12)
      WRITE(6,13)(I,(BS(I,J),J=1,4),I=1,4)
      WRITE(6,14)
      WRITE(6,12)
      WRITE(6,13)(I,(S(I,J),J=1,4),I=1,4)
      WRITE(6,15)
      WRITE(6,12)
      WRITE(6,13)(I,(CM(I,J),J=1,4),I=1,4)
  101 DO 102 I=1,4
      DO 102 J=1,4
      CNE(I,J) = 1.0
  102 CONTINUE
      WRITE(6,16)
      WRITE(6,12)
      WRITE(6,13)(I,(ONE(I,J),J=1,4),I=1,4)

C.. INPUT THE SPECIFIC PROBLEM CASE INFORMATION:

  110 WRITE(6,9)
      READ(5,18)SRATIO,CMU
      DO 111  I=1,9
      READ(5,17)(TITLE(I,J),J=1,60)
      WRITE(6,17)(TITLE(I,J),J=1,60)
  111 CONTINUE
      WRITE(6,19)SRATIO,CMU

C.. FORM TOTAL ELASTIC (A) AND MASS (B) MATRICES:

  120 DO 121 I=1,4
      DO 121 J=1,4
      A(I,J) = BS(I,J) + SRATIO*S(I,J)
      B(I,J) = CONST*(CM(I,J) + CMU*ONE(I,J))
  121 CONTINUE
```

```
.. SOLVE EIGENVALUE PROBLEM USING SUBRCUTINE 'NRCCT'
      CALL NROOT(4,A,B,EV,P)
.. WRITE EIGENVALUES AND CHARACTERISTIC FREQUENCIES:
  130 DO 131 I=1,4
      FREQ(I) = SQRT(EV(I))/(2.0*PI)
  131 CONTINUE
      WRITE(6,20)
      WRITE(6,21)(I,EV(I),FREQ(I),I=1,4)
.. WRITE EIGENVECTORS (MODAL MATRIX):
      WRITE(6,22)
      WRITE(6,12)
      WRITE(6,13)(I,(P(I,J),J=1,4),I=1,4)
.. CALCULATE MODE SHAPE VS. (X/L):
..      X/L = 0.05*(K)
  140 DO 141 K=1,20
      AK = K
      XL(K) = 0.05*AK
      DO 141 I=1,4
      V(I,K) = 0.0
      DO 141 N=1,4
      AN = N
      V(I,K)=V(I,K)+P(N,I)*(1.-COS(((2.*AN)-1.)/40.*PI*AK))
  141 CONTINUE
.. WRITE MODE SHAPE:
      WRITE(6,23)
      WRITE(6,24)
      WRITE(6,25)(K,XL(K),(V(I,K),I=1,4),K=1,20)
      ICASE = ICASE+1
      IF (ICASE.LT.5) GO TO 110
.. FORMAT STATEMENTS:
    9 FORMAT(1H1,////)
   10 FORMAT(4E12.5)
   11 FORMAT(1H1,////,14X,'PITOT-STATIC BOOM ANALYSIS',///,
     1 20X,'INPUT MATRICES',/////,5X,'BEAM STIFFNESS MATRIX,
     2 ',2X,'BS(I,J)',/)
   12 FORMAT(3X,'I/ J=',4X,'1',11X,'2',11X,'3',11X,'4',//)
   13 FORMAT(2X,I2,4F12.5)
   14 FORMAT(/////,4X,'SPRING STIFFNESS INFLUENCE MATRIX,',
     1 2X,'SI,J)',/)
   15 FORMAT(/////,4X,'BEAM MASS MATRIX,CM(I,J)'/)
   16 FORMAT(/////,4X,'TIP MASS INFLUENCE MATRIX, ONE(I,J)'
   17 FORMAT(60A1)
   18 FORMAT(2E12.5)
   19 FORMAT(1H0,5X,'KSP/KB =',F8.5,10X,'MU =',F7.5,//)
   20 FORMAT(1H0,4X,'EIGENVALUES AND MODAL FREQUENCIES ARE:
     1 ',//,3X,'I',4X,'EV(I)',8X,'FREQ.,HZ'/)
   21 FORMAT(2X,I2,2E14.5)
   22 FORMAT(/////,4X,'EIGENVECTORS (MODAL MATRIX) ARE:',/)
   23 FORMAT(/////,4X,'MODE SHAPES VS. X/L ARE:')
   24 FORMAT(1H0,2X,'I',2X,'X/L',7X,'V1(I)',7X,'V2(I)',7X,
     1 'V3(I)',7X,'V4(I)',/)
   25 FORMAT(2X,I2,F6.2,4F12.5)
      STOP
      END
```

PITOT-STATIC BOOM ANALYSIS

INPUT MATRICES

BEAM STIFFNESS MATRIX, BS(I,J)

I/ J=	1	2	3	4
1	1.00000	0.0	0.0	0.0
2	0.0	81.00000	0.0	0.0
3	0.0	0.0	625.00000	0.0
4	0.0	0.0	0.0	2401.CCCCC

SPRING STIFFNESS INFLUENCE MATRIX, S(I,J)

I/ J=	1	2	3	4
1	0.07908	0.46990	0.49592	0.10684
2	0.46990	2.79197	2.94660	0.63482
3	0.49592	2.94660	3.10979	0.66997
4	0.10684	0.63482	0.66997	0.14434

BEAM MASS MATRIX,CM(I,J)

I/ J=	1	2	3	4
1	0.22676	0.57559	0.23606	0.45433
2	0.57559	1.92441	1.08488	1.30315
3	0.23606	1.08488	1.24535	0.96362
4	0.45433	1.30315	0.96362	1.68189

TIP MASS INFLUENCE MATRIX, ONE(I,J)

I/ J=	1	2	3	4
1	1.00000	1.00000	1.00000	1.CCCCC
2	1.00000	1.00000	1.00000	1.00000
3	1.00000	1.00000	1.00000	1.CCCCC
4	1.00000	1.00000	1.00000	1.CCCCC

CASE 1

BASIC BOOM NO SPRING, NO END MASS

KSP/KB = 0.0 MU =0.0

EIGENVALUES AND MODAL FREQUENCIES ARE:

I	EV(I)	FREQ.,HZ
1	0.11793E 08	0.54656E 03
2	0.26594E 07	0.25954E 03
3	0.33621E 06	0.92284E 02
4	0.84605E 04	0.14639E 02

EIGENVECTORS (MODAL MATRIX) ARE:

I/ J=	1	2	3	4
1	-0.87526	0.72915	0.94086	0.99948
2	0.20930	-0.53904	-0.33422	0.03212
3	-0.29252	0.40743	-0.05524	0.00178
4	0.32333	0.10854	-0.00465	0.00084

MODE SHAPES VS. X/L ARE:

I	X/L	V1(I)	V2(I)	V3(I)	V4(I)
1	0.05	0.02846	0.03436	-0.01122	0.00423
2	0.10	0.10290	0.12882	-0.04356	0.01679
3	0.15	0.19409	0.25957	-0.09320	0.03732
4	0.20	0.26430	0.39326	-0.15434	0.06528
5	0.25	0.28017	0.49492	-0.22003	0.10000
6	0.30	0.22448	0.53604	-0.28293	0.14075
7	0.35	0.10316	0.50104	-0.33626	0.18684
8	0.40	-0.05498	0.39059	-0.37438	0.23760
9	0.45	-0.20597	0.22107	-0.39326	0.29244
10	0.50	-0.30372	0.02069	-0.39064	0.35086
11	0.55	-0.31460	-0.17669	-0.36587	0.41236
12	0.60	-0.22913	-0.33838	-0.31971	0.47649
13	0.65	-0.06721	-0.43868	-0.25387	0.54279
14	0.70	0.12520	-0.46242	-0.17070	0.61080
15	0.75	0.28716	-0.40583	-0.07282	0.68009
16	0.80	0.35876	-0.27494	0.03710	0.75026
17	0.85	0.29770	-0.08241	0.15646	0.82096
18	0.90	0.09174	0.15592	0.28276	0.89195
19	0.95	-0.23673	0.42384	0.41362	0.96307
20	1.00	-0.63514	0.70608	0.54675	1.03423

CASE 2

BOOM WITH END MASS NO SPRING

KSP/KB = 0.0 MU =0.68790

EIGENVALUES AND MODAL FREQUENCIES ARE:

I	EV(I)	FREQ.,HZ
1	0.80309E 07	0.45103E 03
2	0.18349E 07	0.21559E 03
3	0.18897E 06	0.69185E 02
4	0.22181E 04	0.74957E 01

EIGENVECTORS (MODAL MATRIX) ARE:

I/ J=	1	2	3	4
1	-0.39361	-0.14964	0.83191	0.99985
2	-0.17520	-0.56564	-0.55293	0.01726
3	-0.38175	0.80552	-0.04587	0.00163
4	0.81771	0.09377	-0.00940	0.00052

MODE SHAPES VS. X/L ARE:

I	X/L	V1(I)	V2(I)	V3(I)	V4(I)
1	0.05	0.08538	0.05905	-0.01759	0.00376
2	0.10	0.31072	0.22364	-0.06859	0.01496
3	0.15	0.59334	0.45873	-0.14795	0.03334
4	0.20	0.82510	0.71393	-0.24801	0.05852
5	0.25	0.90720	0.93362	-0.35952	0.09003
6	0.30	0.78295	1.06804	-0.47276	0.12737
7	0.35	0.45809	1.08273	-0.57852	0.17002
8	0.40	0.00237	0.96478	-0.66896	0.21751
9	0.45	-0.46868	0.72457	-0.73797	0.26939
10	0.50	-0.82657	0.39314	-0.78131	0.32526
11	0.55	-0.96782	0.01599	-0.79644	0.38476
12	0.60	-0.84582	-0.35517	-0.78221	0.44750
13	0.65	-0.48683	-0.67086	-0.73854	0.51310
14	0.70	0.01481	-0.89099	-0.66620	0.58116
15	0.75	0.52151	-0.98962	-0.56672	0.65129
16	0.80	0.89032	-0.95701	-0.44244	0.72306
17	0.85	1.01312	-0.79913	-0.29661	0.79608
18	0.90	0.84770	-0.53541	-0.13341	0.87001
19	0.95	0.43047	-0.19556	0.04199	0.94450
20	1.00	-0.13285	0.18401	0.22370	1.01927

CASE 3

BOOM WITH END MASS AND VERTICAL SPRING

KSP/KB =23.97099 MU =0.68790

EIGENVALUES AND MODAL FREQUENCIES ARE:

I	EV(I)	FREQ.,HZ
1	0.80985E 07	0.45292E 03
2	0.18575E 07	0.21691E 03
3	0.28917E 06	0.85584E 02
4	0.54551E 04	0.11755E 02

EIGENVECTORS (MODAL MATRIX) ARE:

I/ J=	1	2	3	4
1	-0.38433	-0.18127	0.81245	0.99860
2	-0.17941	-0.54894	-0.58231	-0.05228
3	-0.38758	0.80976	-0.02508	-0.00865
4	0.81846	0.10046	-0.01480	0.00044

MODE SHAPES VS. X/L ARE:

I	X/L	V1(I)	V2(I)	V3(I)	V4(I)
1	0.05	0.08496	0.06072	-0.01767	0.00104
2	0.10	0.30908	0.22996	-0.06889	0.00430
3	0.15	0.58982	0.47169	-0.14851	0.01020
4	0.20	0.81920	0.73412	-0.24885	0.01937
5	0.25	0.89872	0.96025	-0.36077	0.03263
6	0.30	0.77198	1.09921	-0.47489	0.05085
7	0.35	0.44505	1.11602	-0.58257	0.07490
8	0.40	-0.01203	0.99784	-0.67662	0.10556
9	0.45	-0.48349	0.75570	-0.75150	0.14336
10	0.50	-0.84076	0.42158	-0.80324	0.18860
11	0.55	-0.98040	0.04189	-0.82908	0.24126
12	0.60	-0.85599	-0.33105	-0.82701	0.30101
13	0.65	-0.49414	-0.64764	-0.79554	0.36725
14	0.70	0.01044	-0.86817	-0.73367	0.43917
15	0.75	0.51975	-0.96745	-0.64112	0.51583
16	0.80	0.89048	-0.93656	-0.51879	0.59624
17	0.85	1.01436	-0.78215	-0.36916	0.67947
18	0.90	0.84913	-0.52392	-0.19665	0.76467
19	0.95	0.43138	-0.19130	-0.00756	0.85109
20	1.00	-0.13285	0.18001	0.19026	0.93811

CASE 4

BOOM WITH END MASS AND HORIZONTAL SPRING

KSP/KB =12.08600 MU =0.68790

EIGENVALUES AND MODAL FREQUENCIES ARE:

I	EV(I)	FREQ.,HZ
1	0.80647E 07	0.45197E 03
2	0.18460E 07	0.21624E 03
3	0.23971E 06	0.77923E 02
4	0.42111E 04	0.10328E 02

EIGENVECTORS (MODAL MATRIX) ARE:

I/ J=	1	2	3	4
1	-0.38896	-0.16524	0.82092	0.99962
2	-0.17732	-0.55750	-0.56978	-0.02709
3	-0.38469	0.80776	-0.03595	-0.00495
4	0.81810	0.09706	-0.01216	0.00048

MODE SHAPES VS. X/L ARE:

I	X/L	V1(I)	V2(I)	V3(I)	V4(I)
1	0.05	0.08517	0.05988	-0.01774	0.00203
2	0.10	0.30990	0.22678	-0.06917	0.00817
3	0.15	0.59158	0.46518	-0.14914	0.01859
4	0.20	0.82215	0.72397	-0.24995	0.03357
5	0.25	0.90296	0.94687	-0.36235	0.05344
6	0.30	0.77746	1.08355	-0.47672	0.07860
7	0.35	0.45156	1.09930	-0.58409	0.10941
8	0.40	-0.00486	0.98123	-0.67690	0.14618
9	0.45	-0.47612	0.74005	-0.74930	0.18911
10	0.50	-0.83370	0.40725	-0.79718	0.23823
11	0.55	-0.97415	0.02878	-0.81788	0.29340
12	0.60	-0.85094	-0.34332	-0.80983	0.35428
13	0.65	-0.49051	-0.65951	-0.77228	0.42033
14	0.70	0.01262	-0.87989	-0.70511	0.49091
15	0.75	0.52064	-0.97888	-0.60898	0.56524
16	0.80	0.89042	-0.94712	-0.48551	0.64257
17	0.85	1.01376	-0.79092	-0.33757	0.72215
18	0.90	0.84843	-0.52986	-0.16949	0.80331
19	0.95	0.43094	-0.19351	0.01300	0.88545
20	1.00	-0.13285	0.18208	0.20302	0.96806

APPENDIX C

CALIBRATION PROCEDURES

Calibration of the data acquisition system should be done about every three months. An ideal time to do the calibration is at the beginning of each academic quarter. A majority of the work can be done on the aircraft, but it may be necessary to remove some system components in order to calibrate them. Only minor adjustments should be necessary during these periodic calibrations. Calibration procedures are outlined below:

A. DIGITAL VOLTMETERS

The voltmeters may be removed from the aircraft and calibrated in the lab, or they may be calibrated while mounted in the consoles. If it is desired to remove the meter from the console, proceed with step 1; otherwise, start with step 2.

1) Unsnap the plastic cover from the face of the meter and remove the four mounting screws which hold the meter in the console. Lift the meter out of the console.

2) Unplug the connector plug from the rear of the meter.

3) A connector plug with dummy leads is available in the Aeronautics Department Electronic Shop. Plug this connector into the meter.

4) Power for the meter is obtained by connecting pin 18A of the connector plug to +5VDC, and pin 18B to ground (-5VDC).

5) Ground pin 14A. If all of the segments of the meter display are working correctly, a reading of +1.888 should appear.

After a five minute warmup, proceed as follows:

BALANCE CONTROL

6) Short the analog input terminals (pins A18 and B18) to analog common (pin B4).

7) Rotate the balance control (see Figure 21) until the display is flickering between (+) zero and (-) zero.

ZERO CONTROL

8) Connect a precision voltage reference source to the analog input terminals (pins 18A and 18B).

9) Adjust the voltage output from the reference source to 300 micro-volts. Rotate the zero control (see Figure 21) until the least significant digit of the meter display flickers between zero and one.

FULL SCALE CONTROL

10) Adjust the output from the reference source to 1.990 volts. Rotate the full scale control of the panel meter (see Figure 21) until the meter display reads 1.990 volts.

B. POSITION INDICATORS

Two people will be required to complete this phase of the calibration.

1) Physically position each control surface in its neutral position and zero the output signal of each circuit by adjusting its balance potentiometer.

2) Place a clinometer on the right aileron. Adjust the trailing edge of the aileron over the range ±20 degrees from the neutral position in increments of five degrees. Compare the output at each angle with the initial calibration curve and note any significant differences.

3) Place the clinometer on the elevator and adjust the trailing edge over a range of 25 degrees up to 15 degrees down in increments of five degrees. Compare the output with the initial calibration curve and note significant differences.

4) A special protractor is available for use in calibrating the rudder position transducer. Place this protractor between the rudder and the fuselage and ensure that the centerline of the protractor coincides with the centerline of the vertical stabilizer. Adjust the trailing edge of the rudder through the range ±25 degrees in increments of five degrees. Compare the output with the initial calibration curve and note significant differences.

C. YAPS HEAD

1) Position the sideslip vane in the neutral position by aligning the scribe marks on the vane shaft. Zero the output signal using the sideslip balance potentiometer on the junction box.

2) Using a protractor, adjust the vane through the range ±20 degrees in increments of five degrees. Compare the output signal with the initial calibration curve and note any significant differences.

3) Repeat 1) and 2) above for the angle of attack vane.

D. FORCE INDICATORS

Calibration of the force indicators consists of ZERO and GAIN adjustments to the appropriate operational amplifiers.

1) Ensure that the copilot's yoke is free. Place the control lock on the pilot's control column.

2) Zero the elevator force signal by adjusting the ZERO screw in the ELEVATOR FORCE operational amplifier.

3) Using a hand-held force gage, or a weight and pulley arrangement, apply a 10-pound nose-up force to one side of the copilot's control wheel. Adjust the GAIN of the op amp until an output signal of +150 millivolts is obtained. Next, recheck the zero reading. Several iterations may be required to establish the proper ZERO/GAIN adjustment. Now apply several different force increments in both the nose-up and nose-down directions to ensure that the output signal matches the original calibration data. If significant differences exist, it may be necessary to do a more careful calibration and create a new data reduction curve.

4) Repeat 2) and 3) for the AILERON FORCE operational amplifier. Application of a 10-pound force in the right wing down direction should be adjusted to read +150 millivolts. Again, check that forces in both directions create an output comparable to original calibration data.

5) There are two operational amplifiers associated with the rudder force circuit, and it is necessary to adjust each one separately. Remove the left cannon plug from the RT

RUDDER FORCE op amp. Using an external power supply, patch +28 VDC into pin C and -28 VDC into pin B of the operational amplifier. Next, patch pin E into the high side of a digital voltmeter, and pin D into the low side. Adjust the ZERO screw on the op amp to obtain a zero signal. Remove the right rudder force transducer from the rudder pedal and place it upright on the cockpit floor. Place a ten-pound weight on the transducer, and adjust the GAIN screw to obtain an output signal of +100 millivolts. As before, several attempts may be necessary to obtain the proper balance between the ZERO and GAIN adjustments. Apply several different forces to the transducers to check for agreement with original calibration data. Replace the cannon plug when complete.

6) Repeat 5) for the LEFT RUDDER FORCE op amp.

7) In order to calibrate the accelerometer operational amplifier, it will be necessary to remove the accelerometer from its mount. Place the accelerometer on its back and, with the help of a bubble-type level, make sure that the sensing axis is exactly horizontal. Zero the output signal by adjusting the ZERO screw on the accelerometer op amp. Next place the accelerometer upright (sensing axis exactly vertical) and adjust the GAIN screw to obtain an output of +500 millivolts. Once the proper GAIN/ZERO balance has been found, the accelerometer should read +500 millivolts when upright, zero millivolts when on its back, and -500 millivolts when upside down.

APPENDIX D

PREFLIGHT PROCEDURES

Before each flight, it should be decided which electrical transducers will be used for that flight. Preflight adjustment is necessary only for those transducers that will be utilized.

1) Using jumper wires, connect the desired sensor input plugs to output plugs on the junction box. (Ensure that red input plugs are connected to red output plugs, and black input is connected to black output). Make a note of which input sensor is connected to which output channel. If more than five electrical sensors are required for the flight, it will be necessary to switch the jumper wires in flight.

2) Check all plugs/cables connected and tight.

After the pilot has completed his cockpit preflight, proceed as follows:

3) Turn on the aircraft battery switch.

4) Turn on the main power supply switch located on the data acquisition system junction box.

5) If the rudder force sensors will be used in flight, turn on the rudder force summer switch. Otherwise, leave it in the off position. (This switch is located next to the power supply switch).

If the flight control surface position indicators are to be used:

6) Station someone at the rudder to hold it in the neutral position. Loosen the locking nuts on the rudder balance pot shaft and zero the rudder position signal. Hold the pot shaft in place and retighten the locking nuts. Check to see that movement of control surface results in change in the digital output signal.

7) Repeat 6) for elevator.

8) Repeat 6) for aileron.

If control force indicators are to be used:

9) Ensure that the copilot's control wheel is free.

10) Using a small jeweler's screwdriver, rotate the ZERO adjusting screw on the op amp marked ELEVATOR. (This adjustment is very sensitive and an exact zero may not be possible. Note any error in the zero position). Do not touch the GAIN screw - this adjustment is made during periodic system calibration. Ensure that a force applied to the copilot's wheel in the fore and aft direction results in a change in the digital readout for elevator force.

11) Repeat 10) for AILERON op amp.

12) Ensure that the rudder force transducer blocks are mounted on the copilot's rudder pedals. Exercise these transducers to ensure that a force applied to the right rudder results in a positive signal and a force applied to the left rudder pedal results in a negative signal. No zero adjustment should be attempted - note the zero force reading and apply this as a correction to any reading taken in flight.

If the YAPS head is to be used in flight:

13) Position the AOA vane in the neutral position by aligning the scribe marks on the vane shaft. Loosen the locking nuts on the AOA balance pot shaft and zero the AOA signal. Hold the shaft in place and retighten the locking nuts. Check that movement of the AOA vane results in a corresponding change in the AOA signal.

14) Repeat 13) for the sideslip vane.

If the accelerometer is to be used in flight:

15) Check for an output signal of approximately 500 millivolts. No preflight adjustments are possible. If signal is in extreme error, accelerometer op amp must be calibrated in accordance with Appendix C.

Pitot-static Systems

It is possible to select which pitot-static system is connected to each console altimeter/airspeed indicator. Connections are accomplished with quick disconnect fittings at the pitot-static selector panel located on the rear of the right front seat.

16) Connect each set of pitot-static lines to the input lines for the desired instrument console. Note which system is connected to each console.

17) Check to see that all pitot-static ports are clear and unobstructed.

18) Set the correct barometric pressure in the window of each console altimeter.

POSTFLIGHT PROCEDURES

1) Turn off the power supply switch and the rudder summer switch.

2) Install the vane guard on the YAPS head.

3) Note any system discrepancies.

APPENDIX E

FIGURES

FIGURE 1. CESSNA 310H, N164X

FIGURE 2. REMOTE-SENSING PITOT-STATIC BOOM

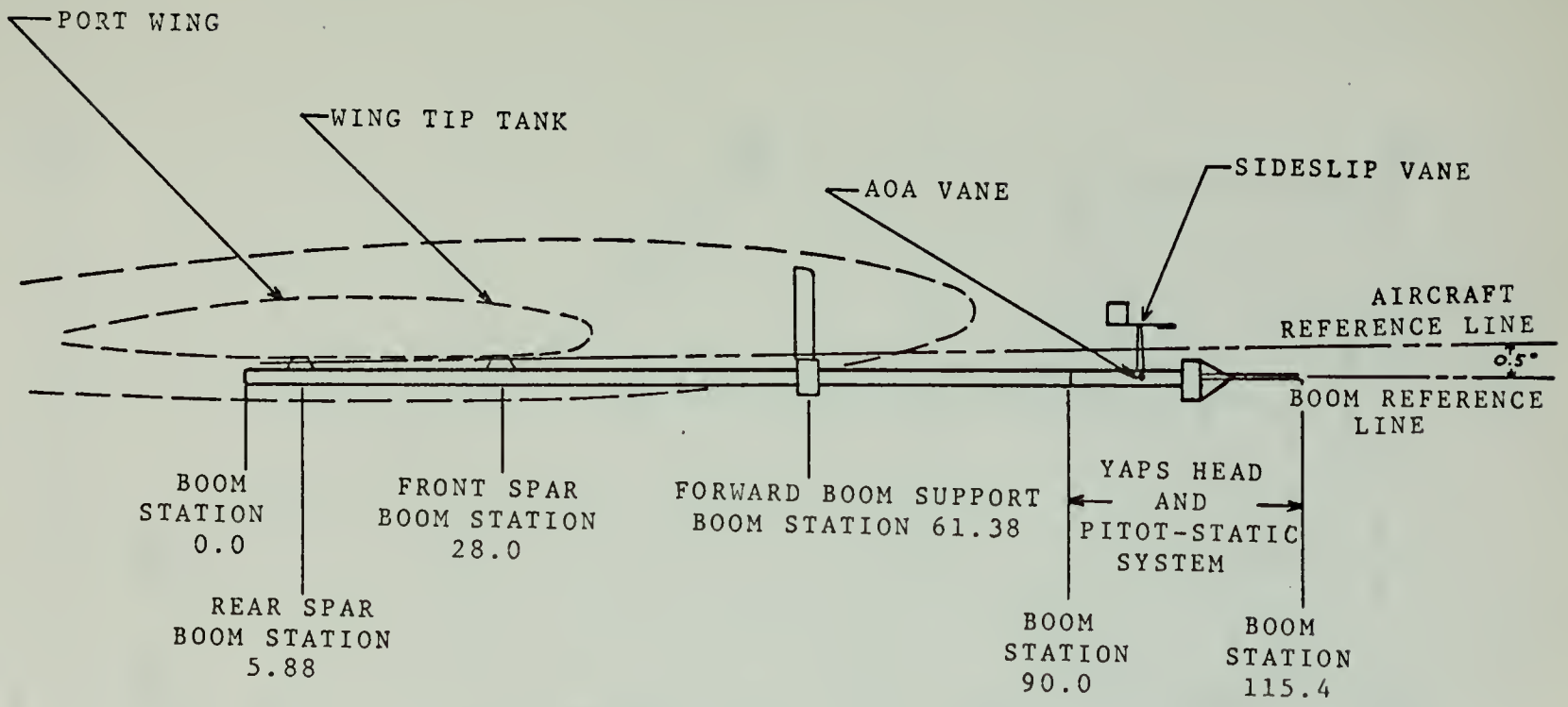

FIGURE 3. PITOT-STATIC BOOM DIMENSIONS

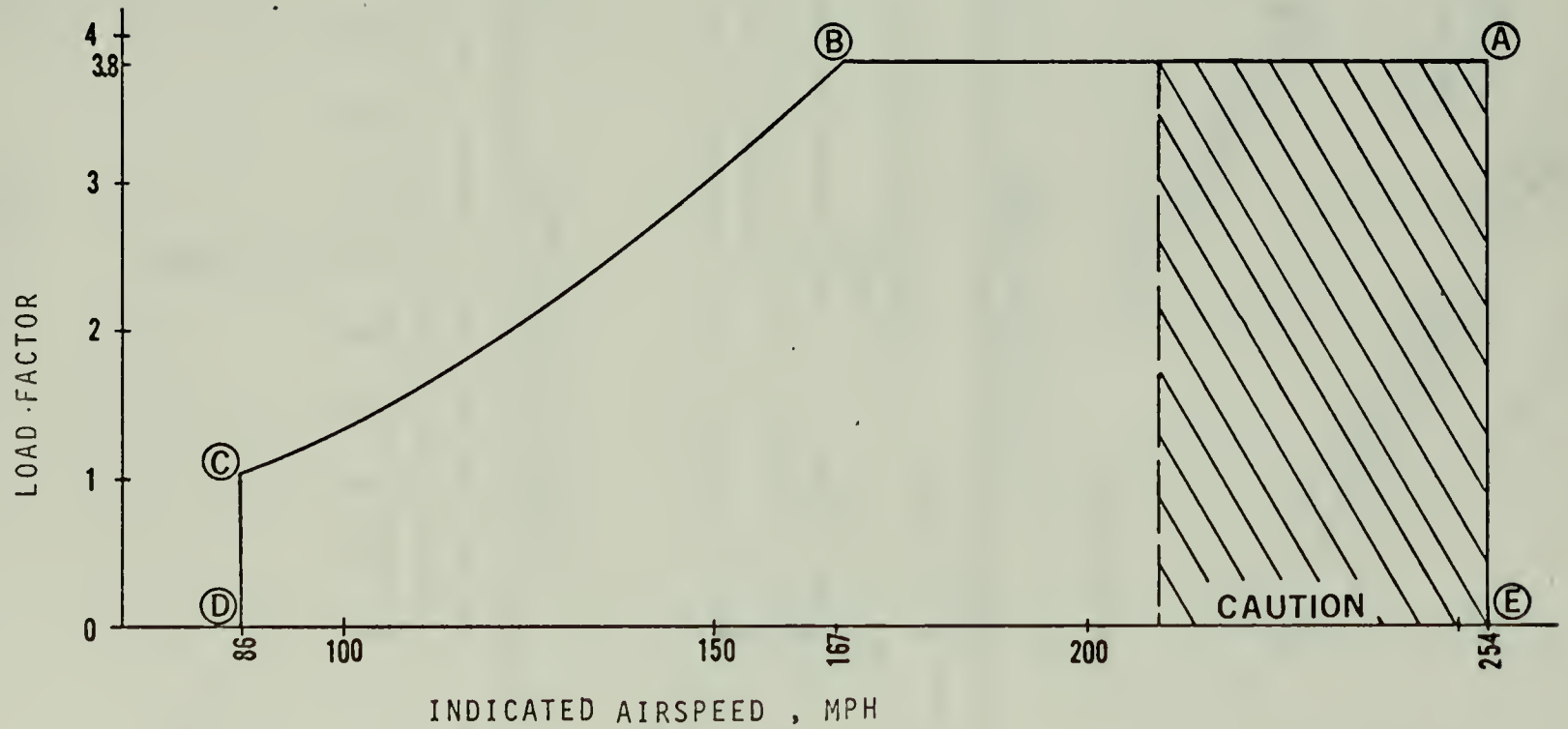

FIGURE 4. V-n DIAGRAM

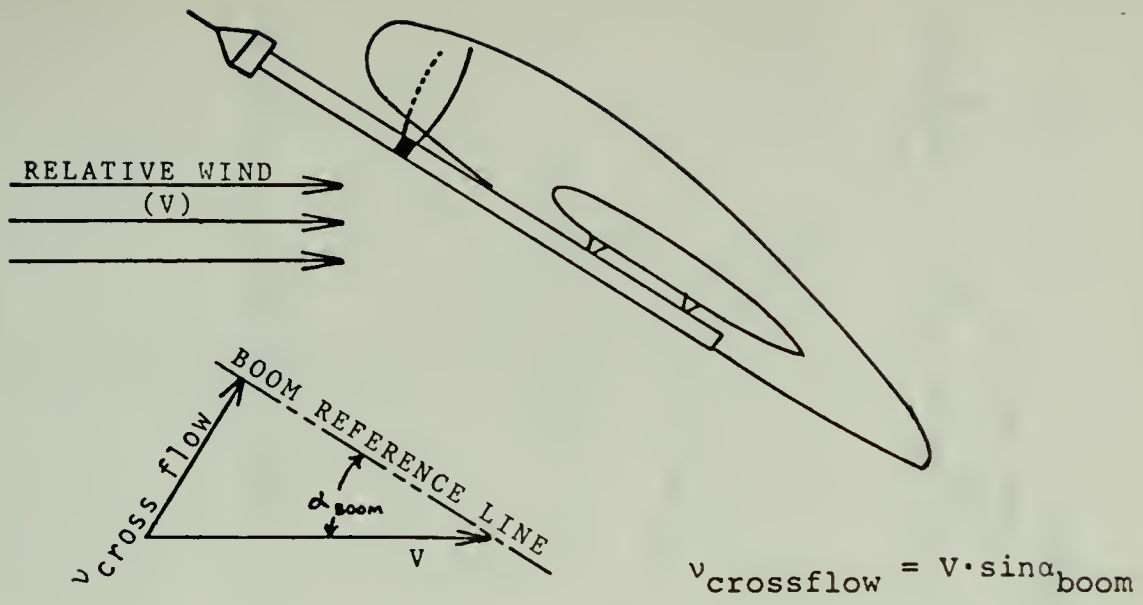

FIGURE 5. CROSSFLOW VELOCITY

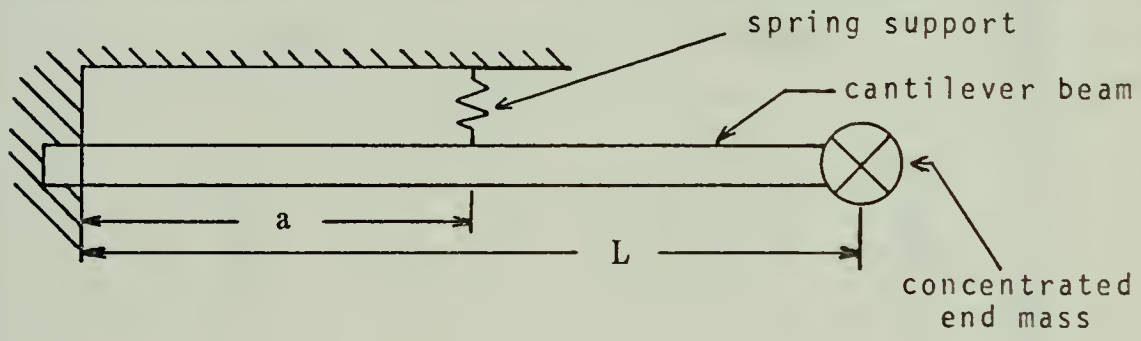

FIGURE 6. THEORETICAL BOOM MODEL

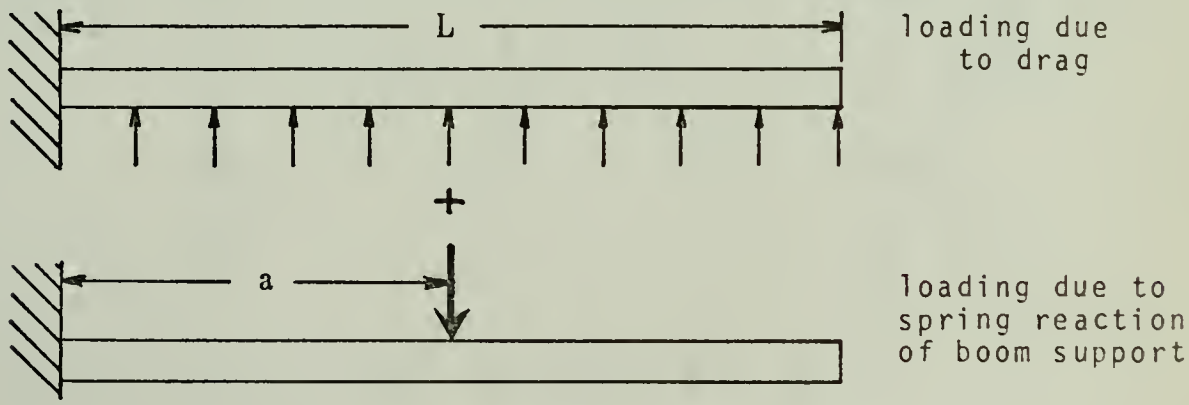

FIGURE 7. BOOM LOADING

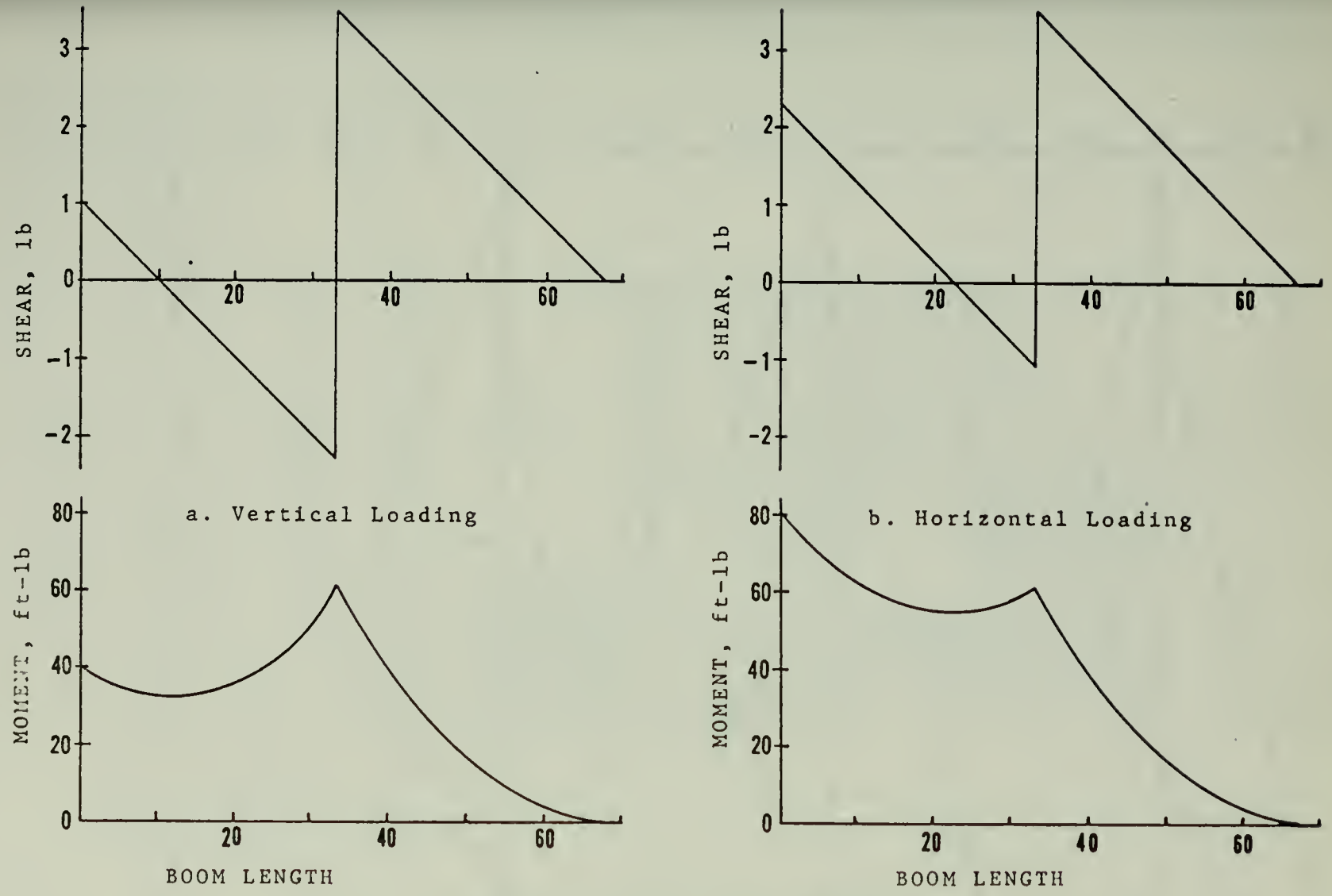

FIGURE 8. BOOM SHEAR AND MOMENT DIAGRAMS

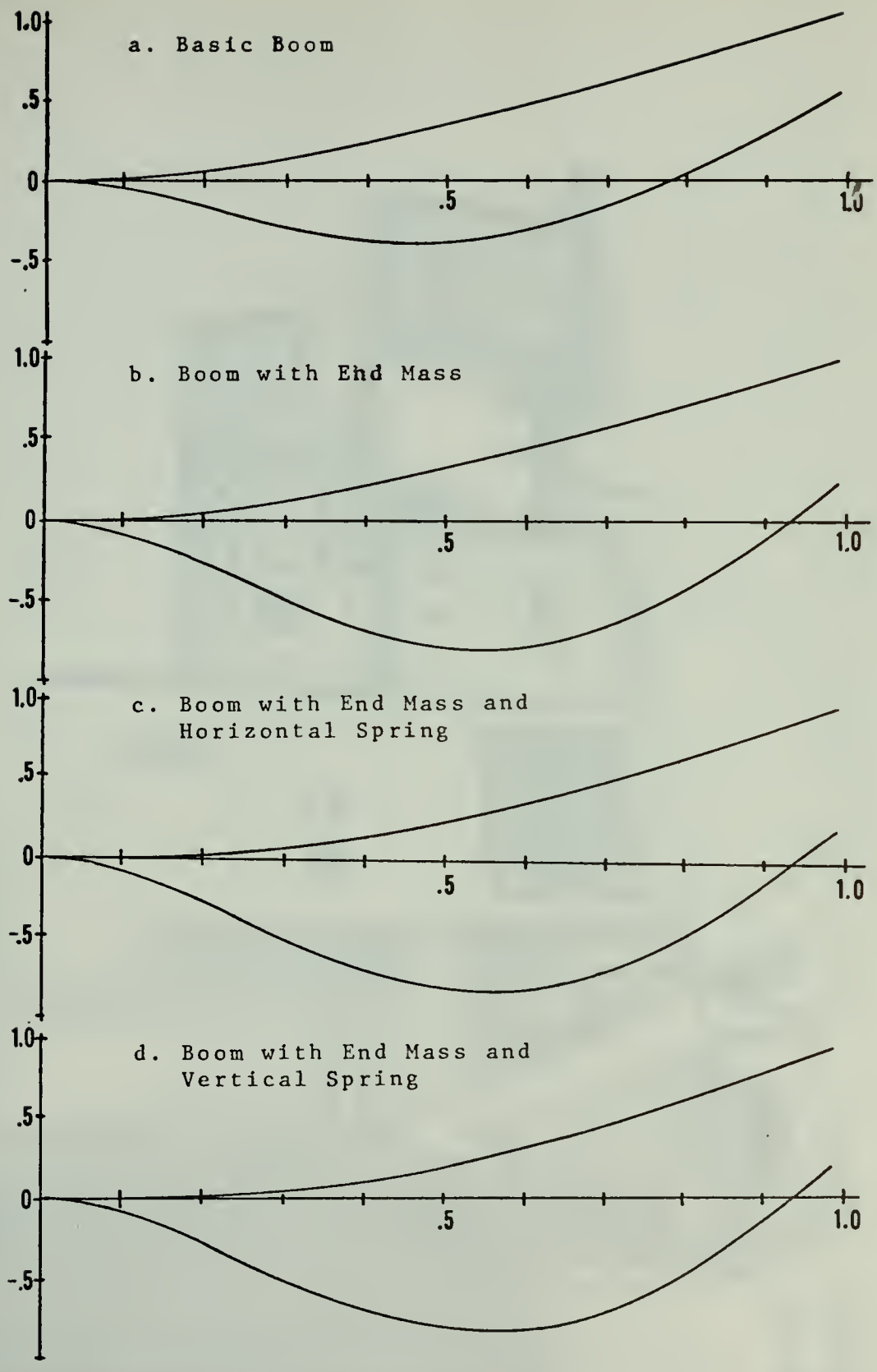

FIGURE 9. NORMALIZED BOOM MODE SHAPES

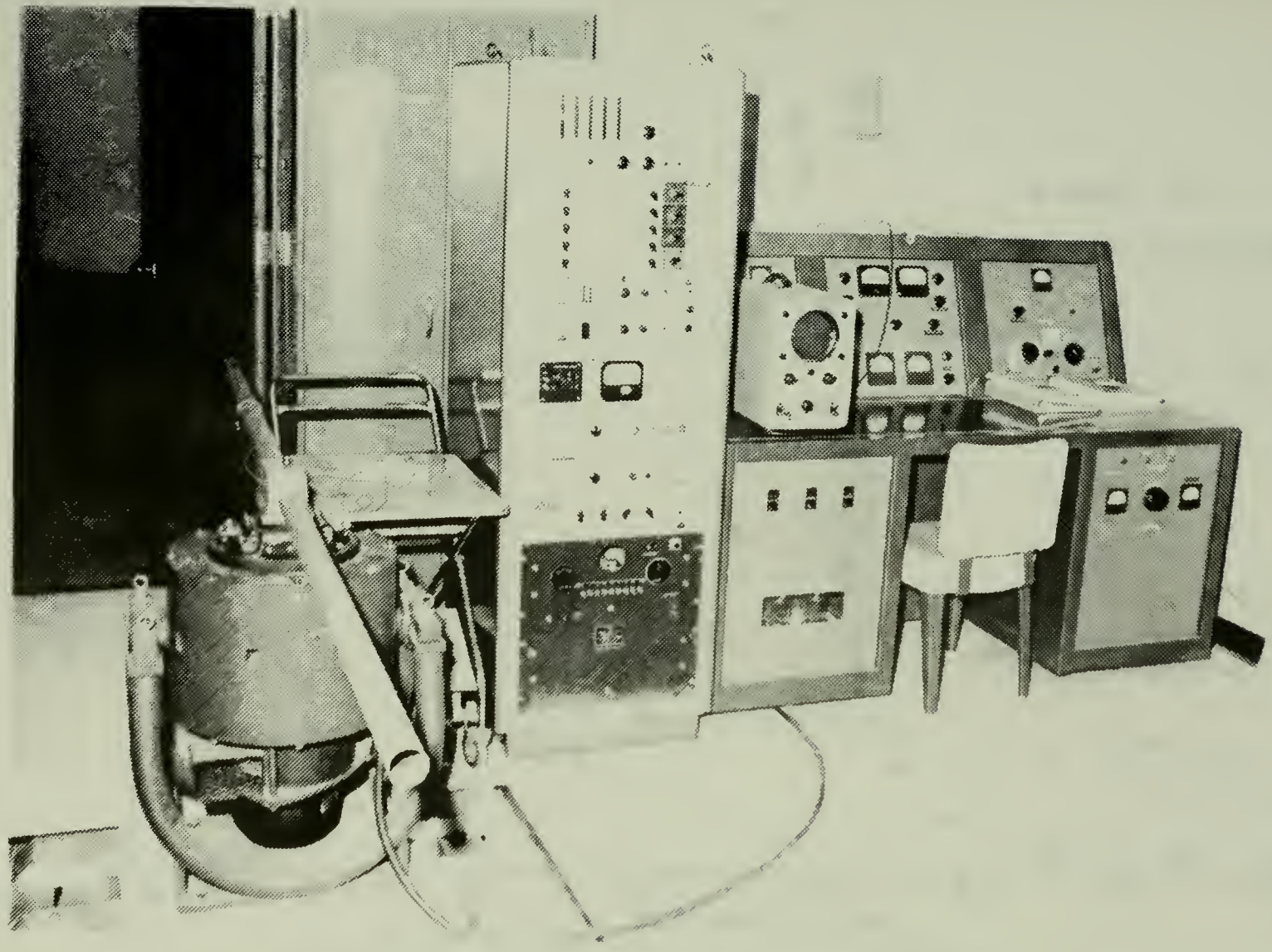

FIGURE 10. SHAKER TABLE SET-UP

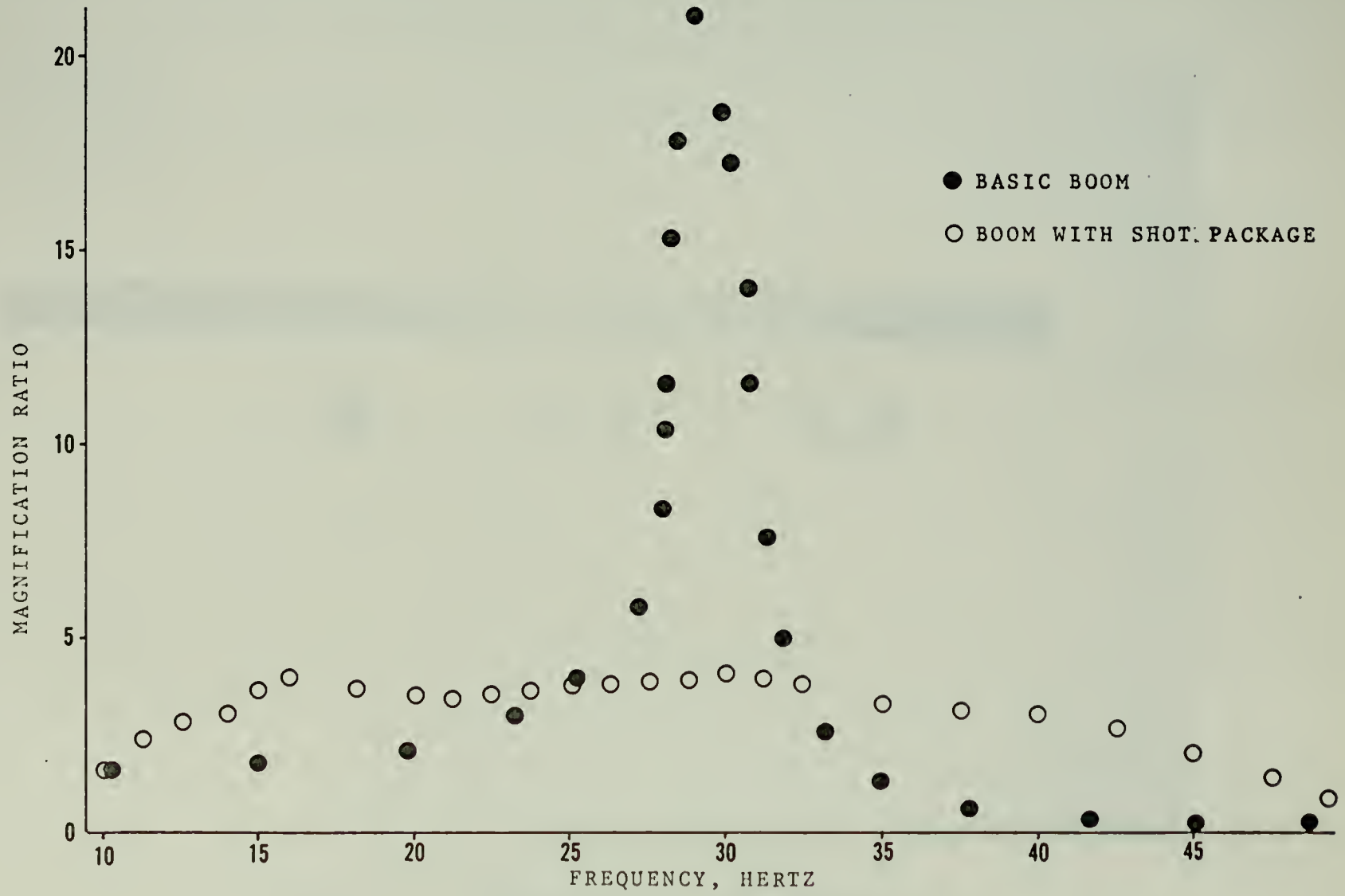

FIGURE 11. COMPARISON OF FIRST MODE SHAPE WITH AND WITHOUT SHOT

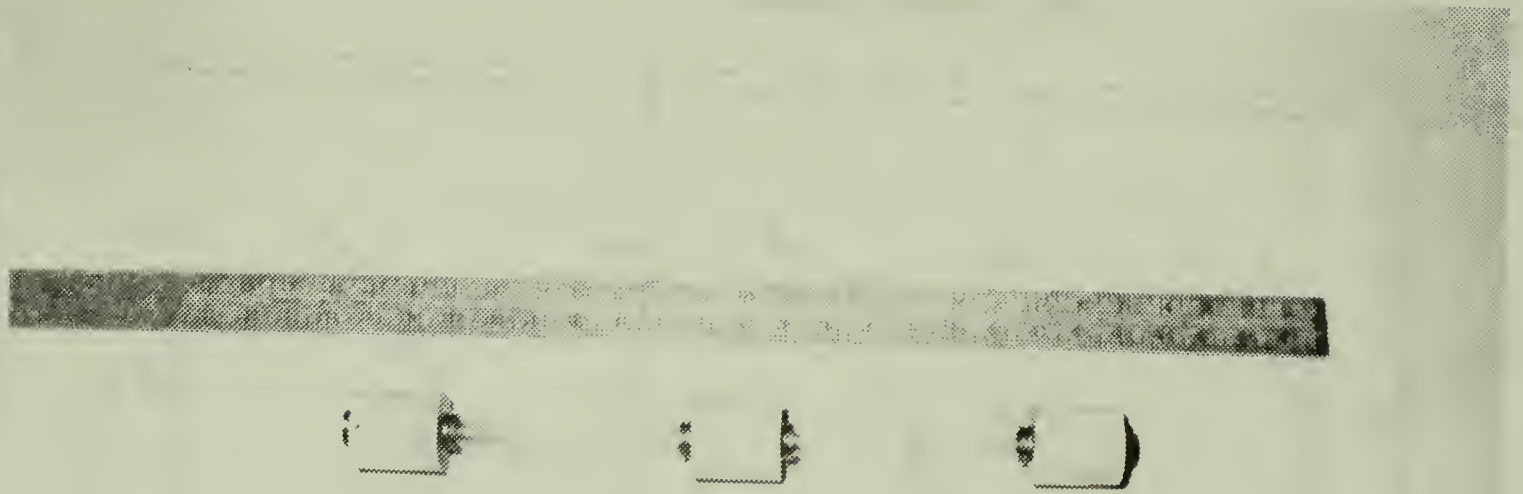

FIGURE 12. BOOM MODEL SHOT COMPARTMENTS

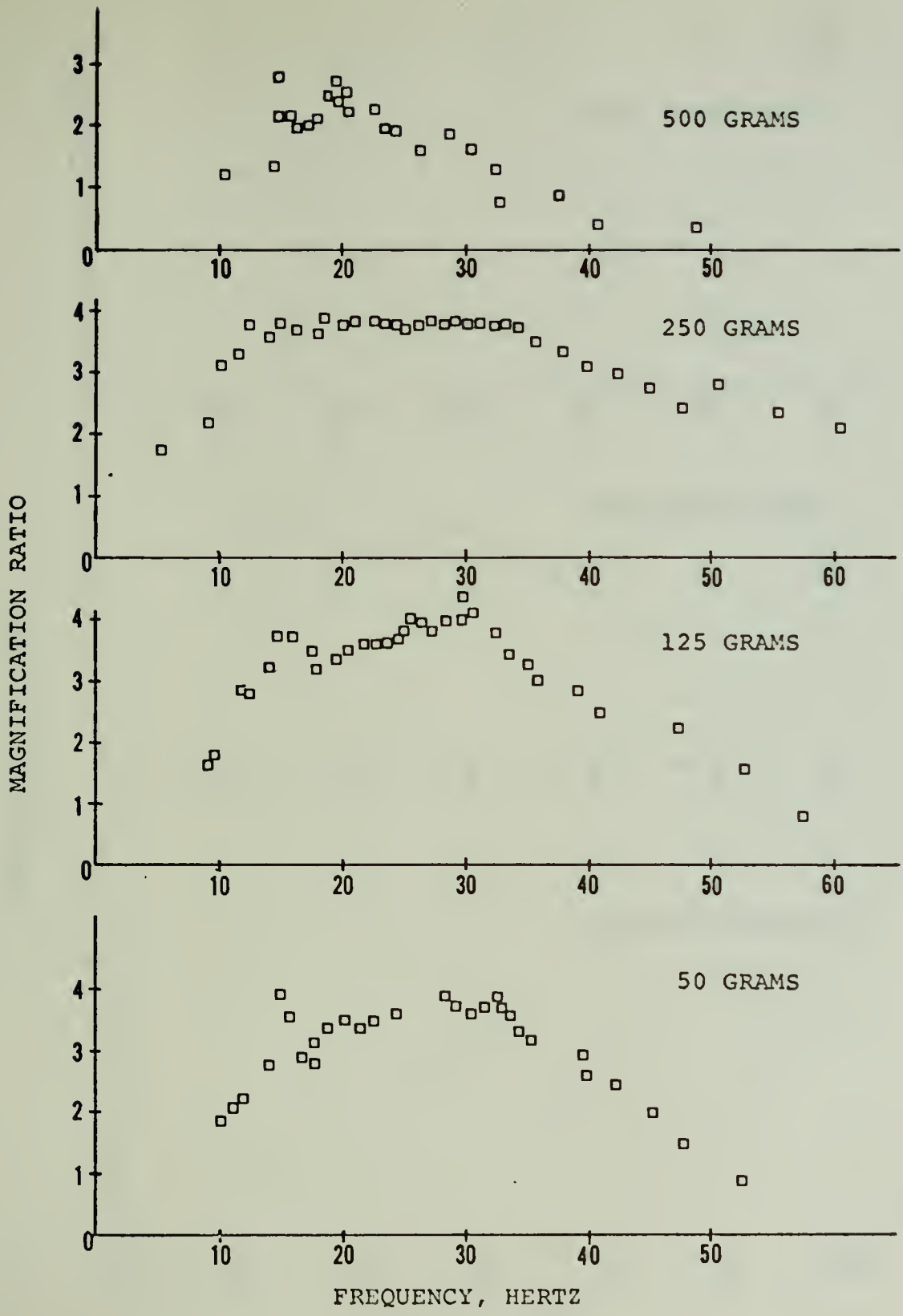

FIGURE 13. EFFECT OF VARYING AMOUNT OF SHOT IN BOOM MODEL

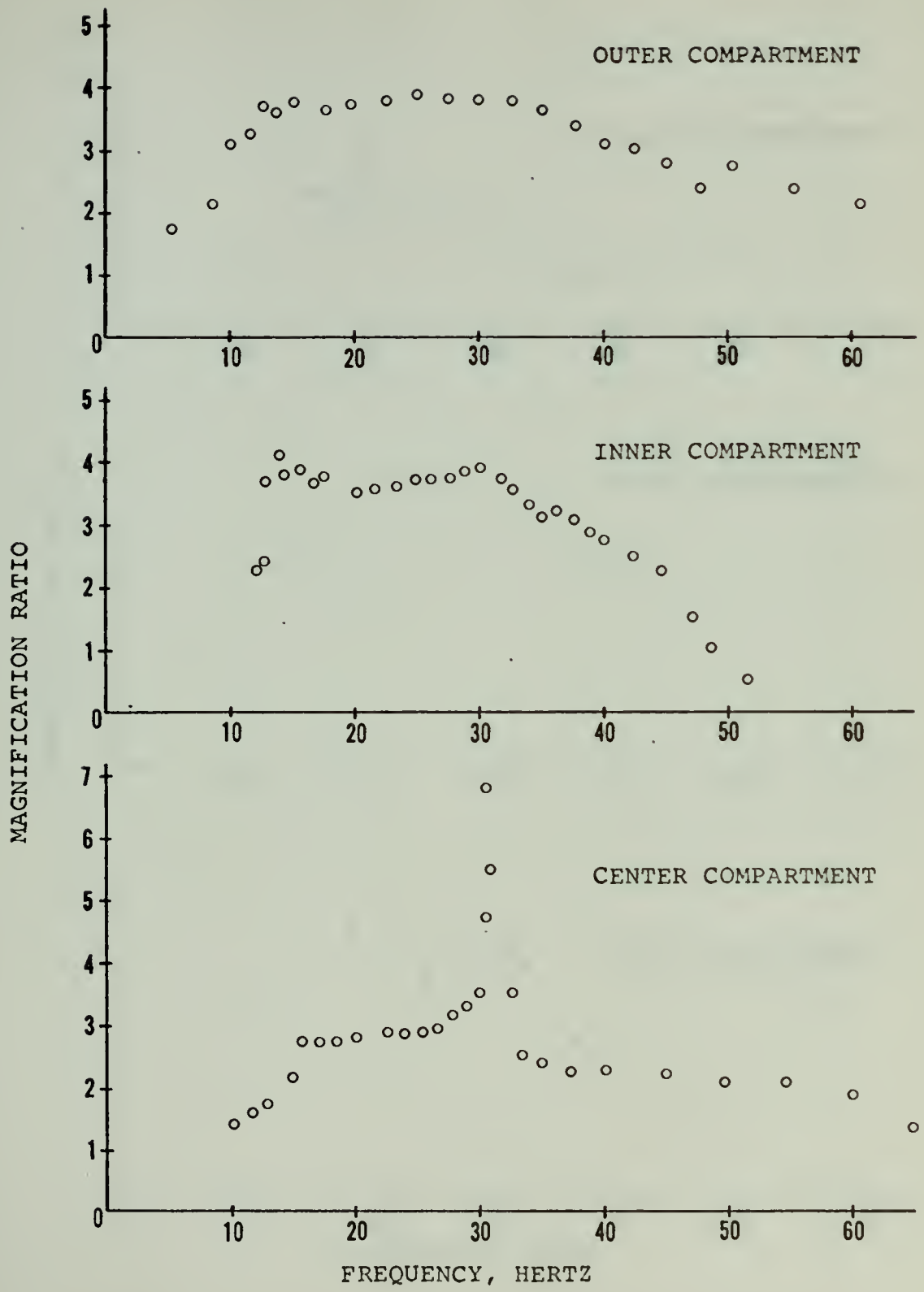

FIGURE 14. EFFECT OF VARYING LOCATION OF SHOT COMPARTMENT

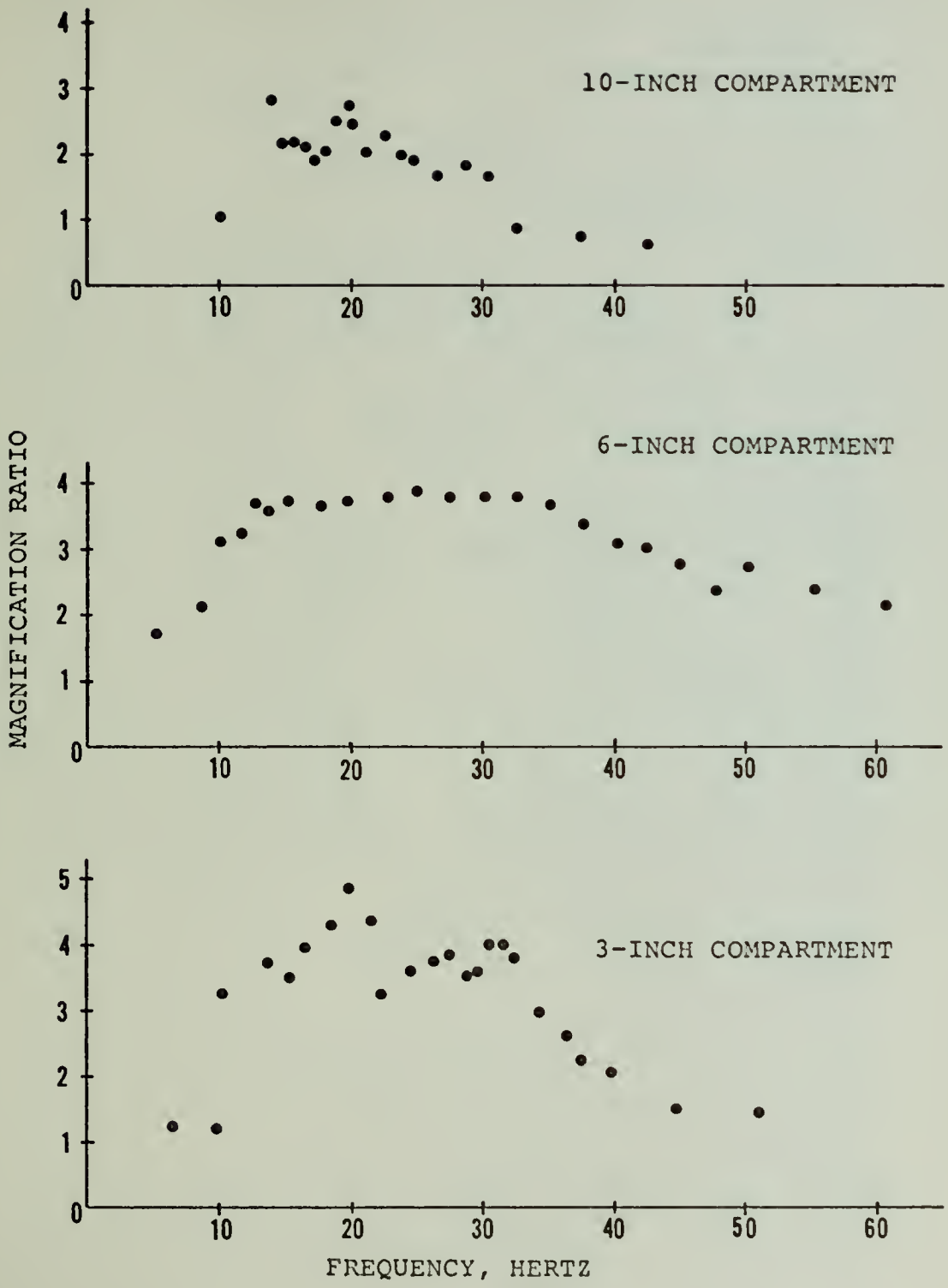

FIGURE 15. EFFECT OF VARYING SIZE OF SHOT COMPARTMENT

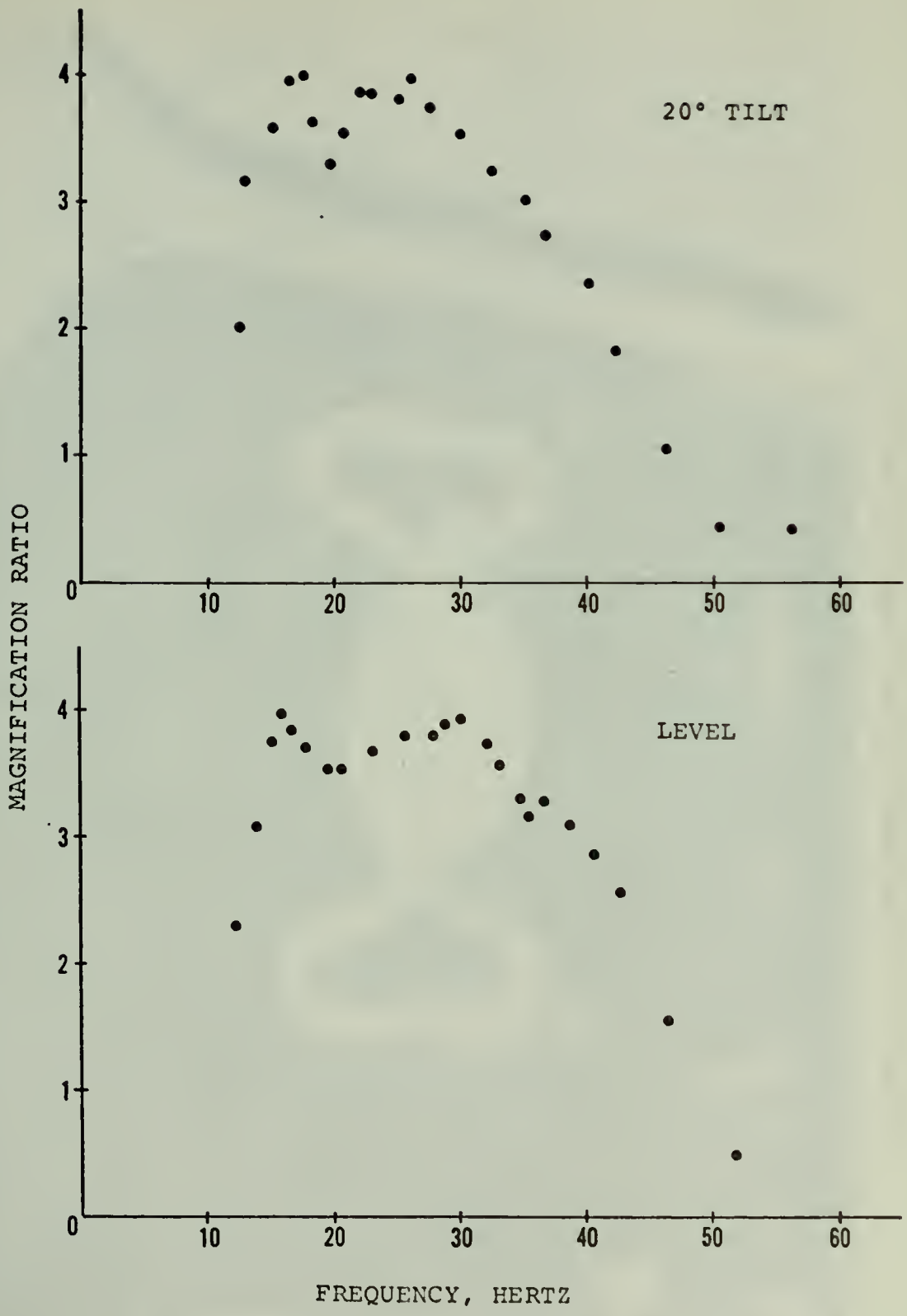

FIGURE 16. EFFECT OF TILTING SHOT COMPARTMENT

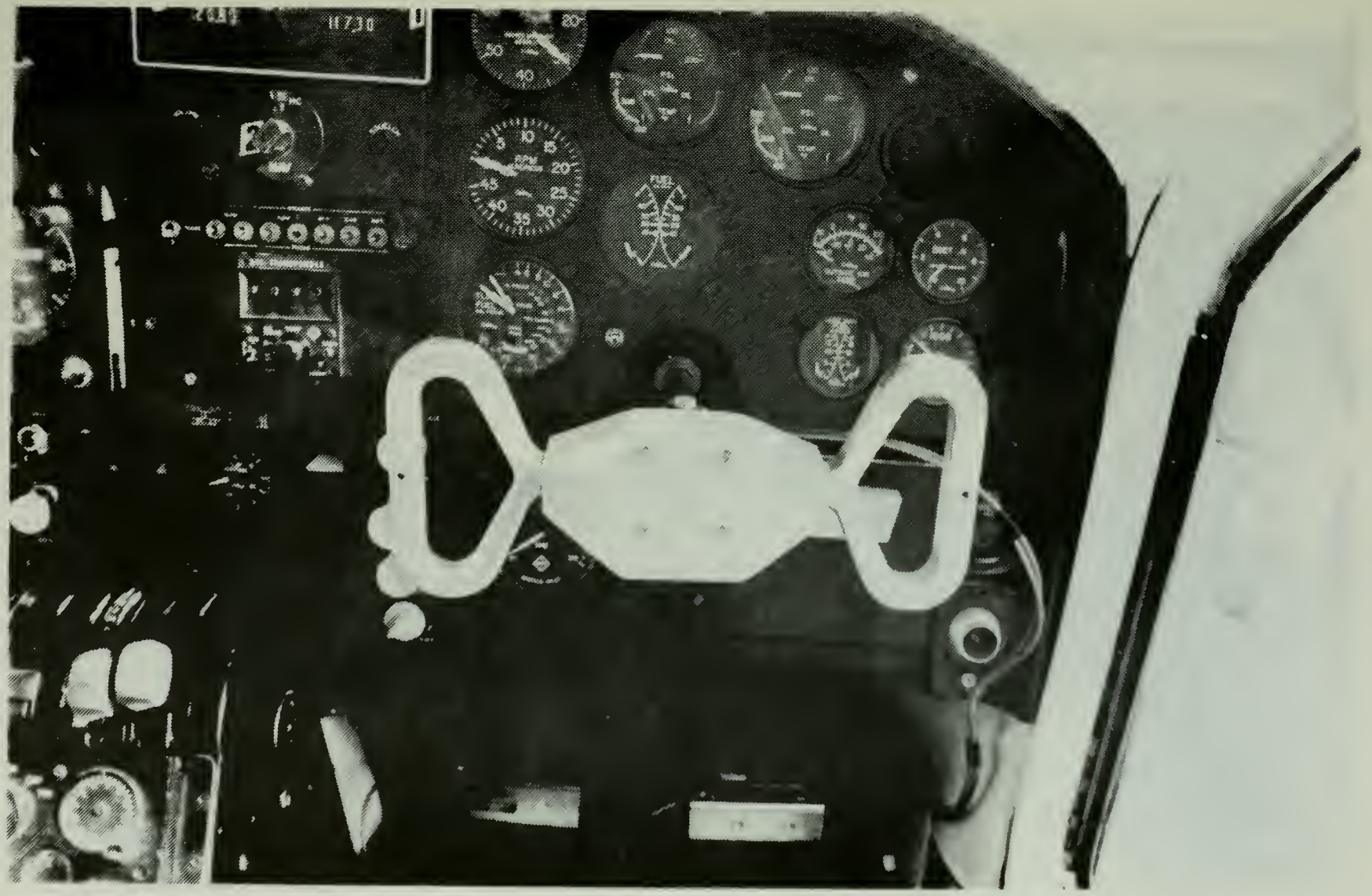

FIGURE 17. INSTRUMENTED CONTROL WHEEL INSTALLATION

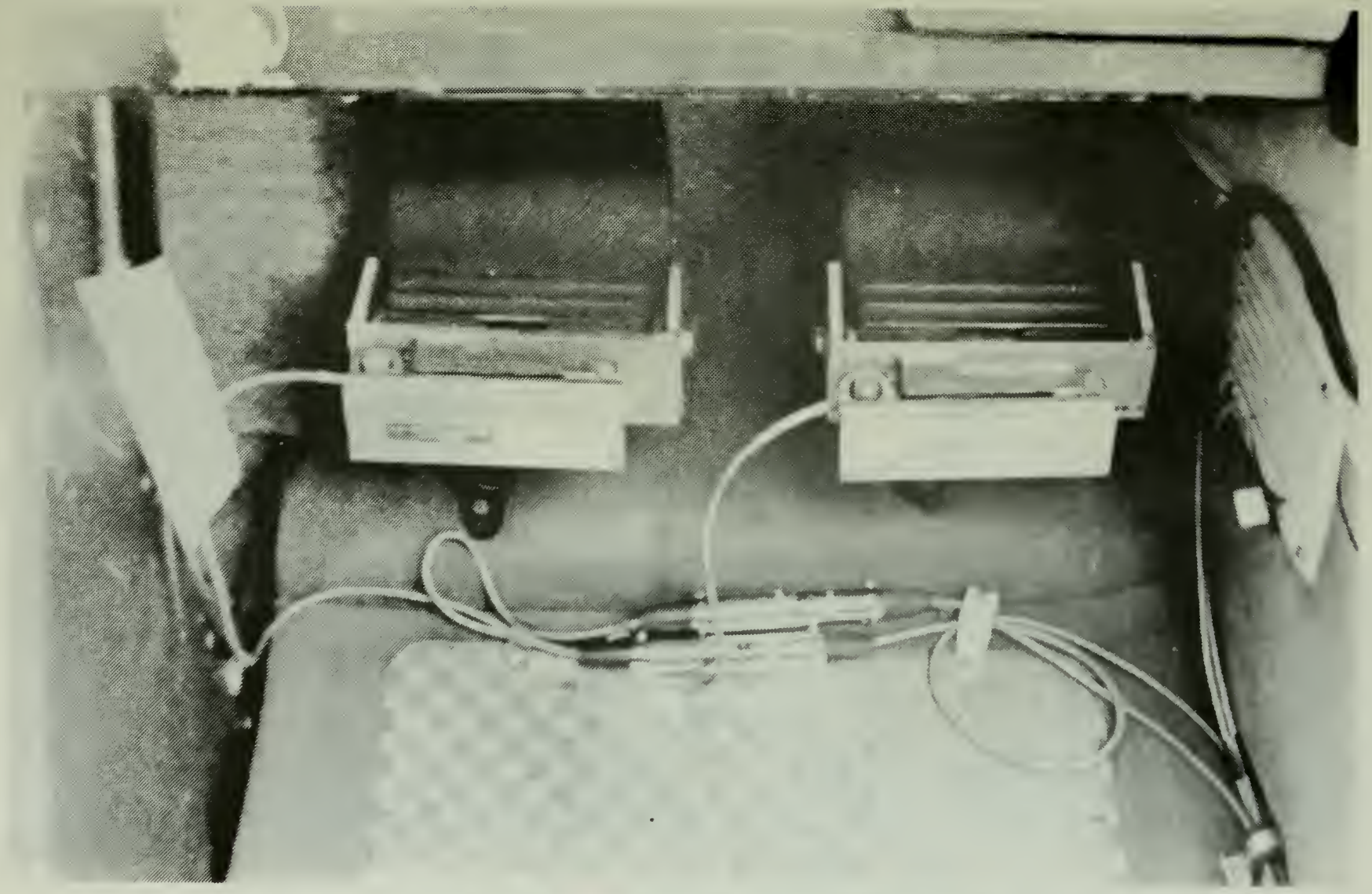

FIGURE 18. RUDDER PEDAL FORCE TRANSDUCER

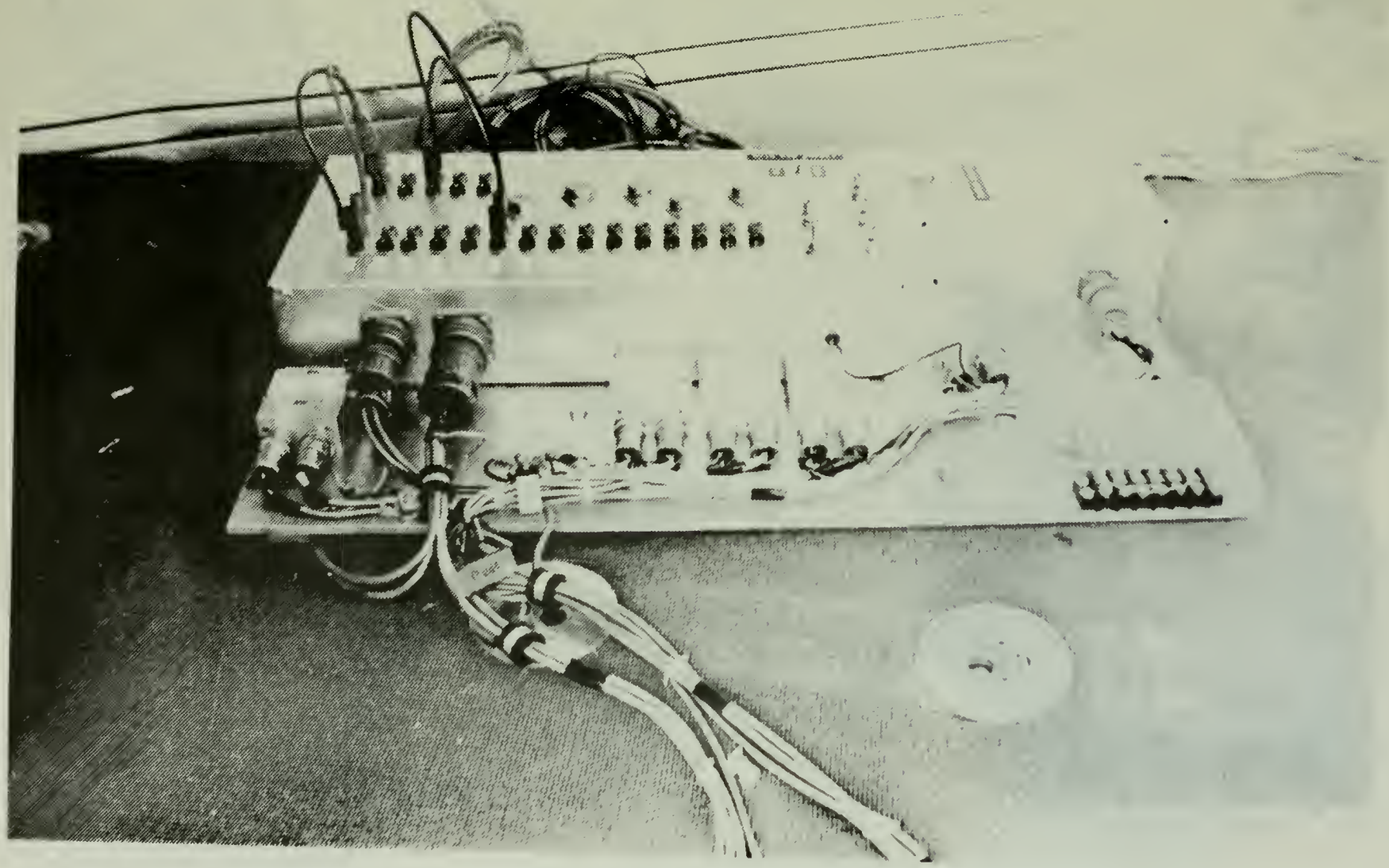

FIGURE 19. JUNCTION BOX AND SIGNAL CONDITIONING INSTALLATION

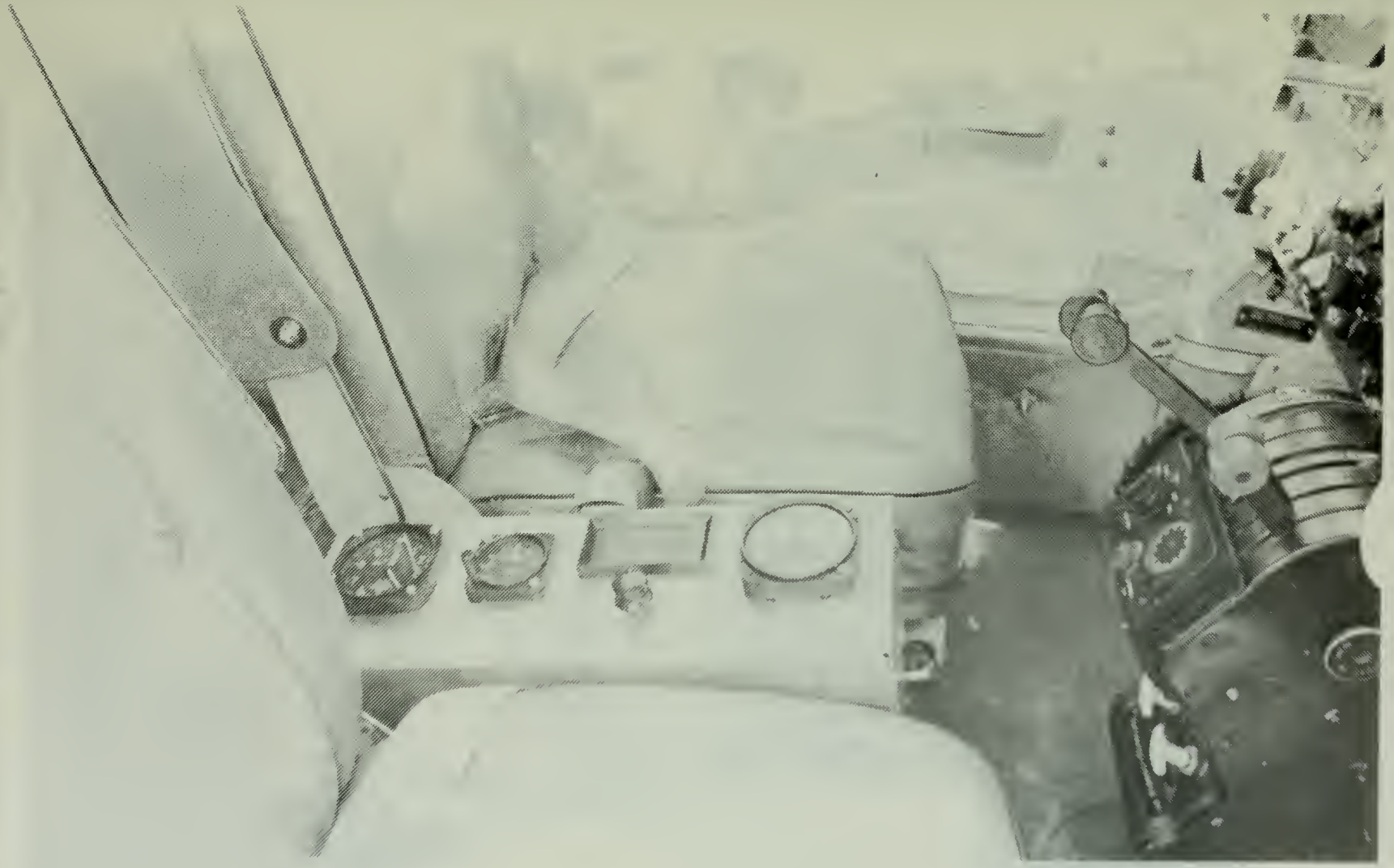

FIGURE 20. INSTALLATION OF COPILOT'S INSTRUMENT CONSOLE

a. Mounted

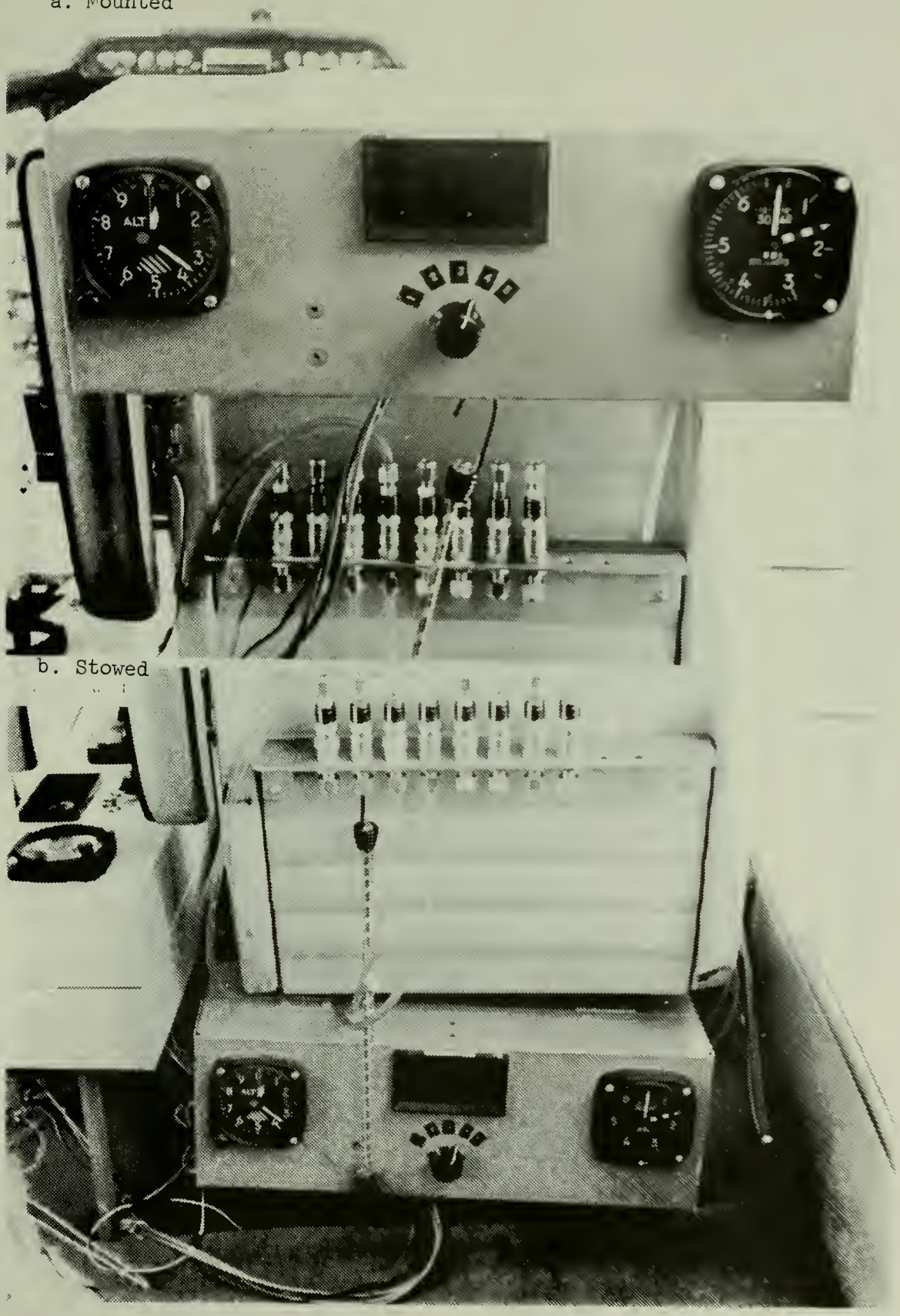

b. Stowed

FIGURE 21. INSTALLATION OF REAR SEAT INSTRUMENT CONSOLE

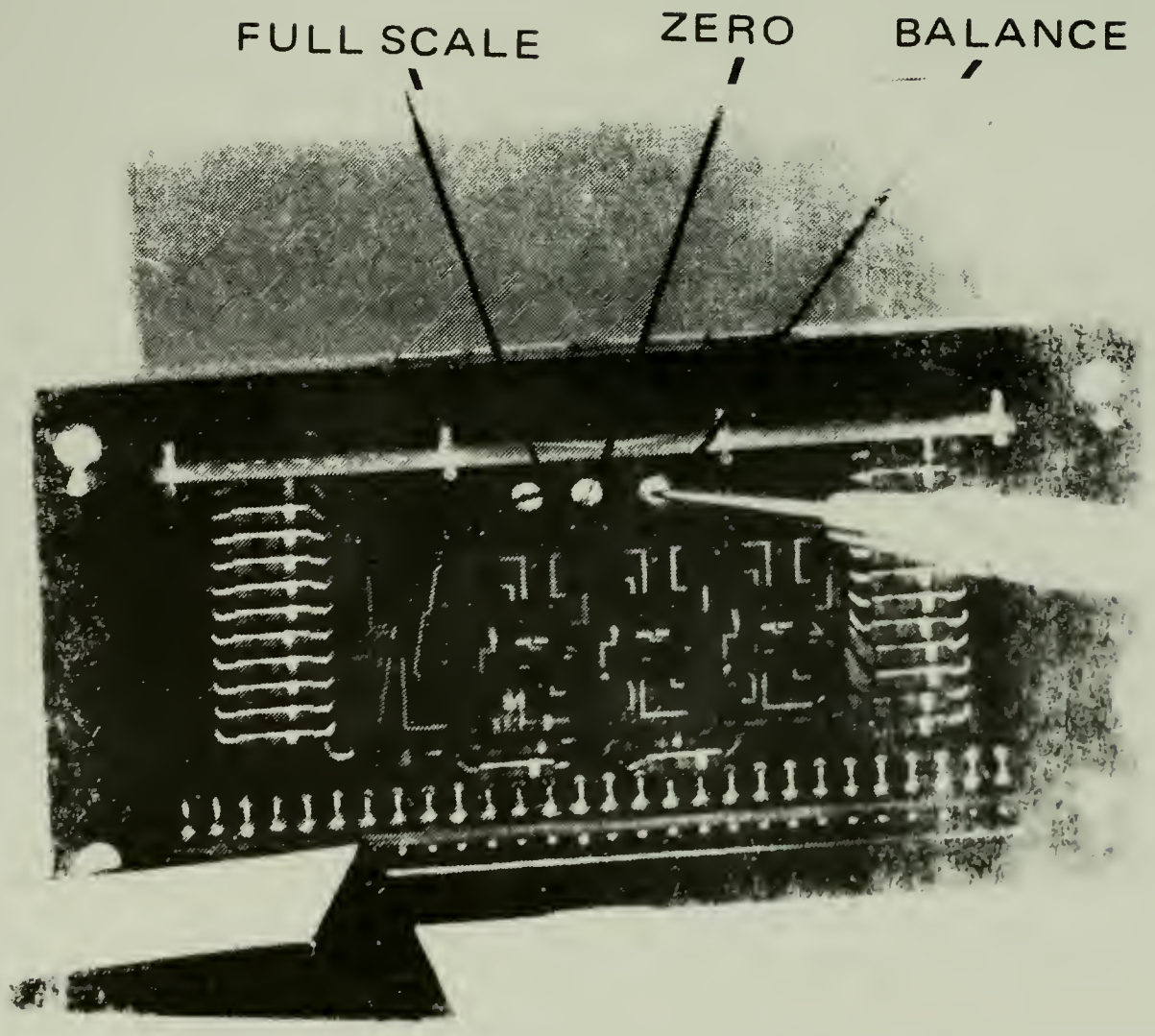

FIGURE 22. DATEL 1000 ADJUSTMENT CONTROLS

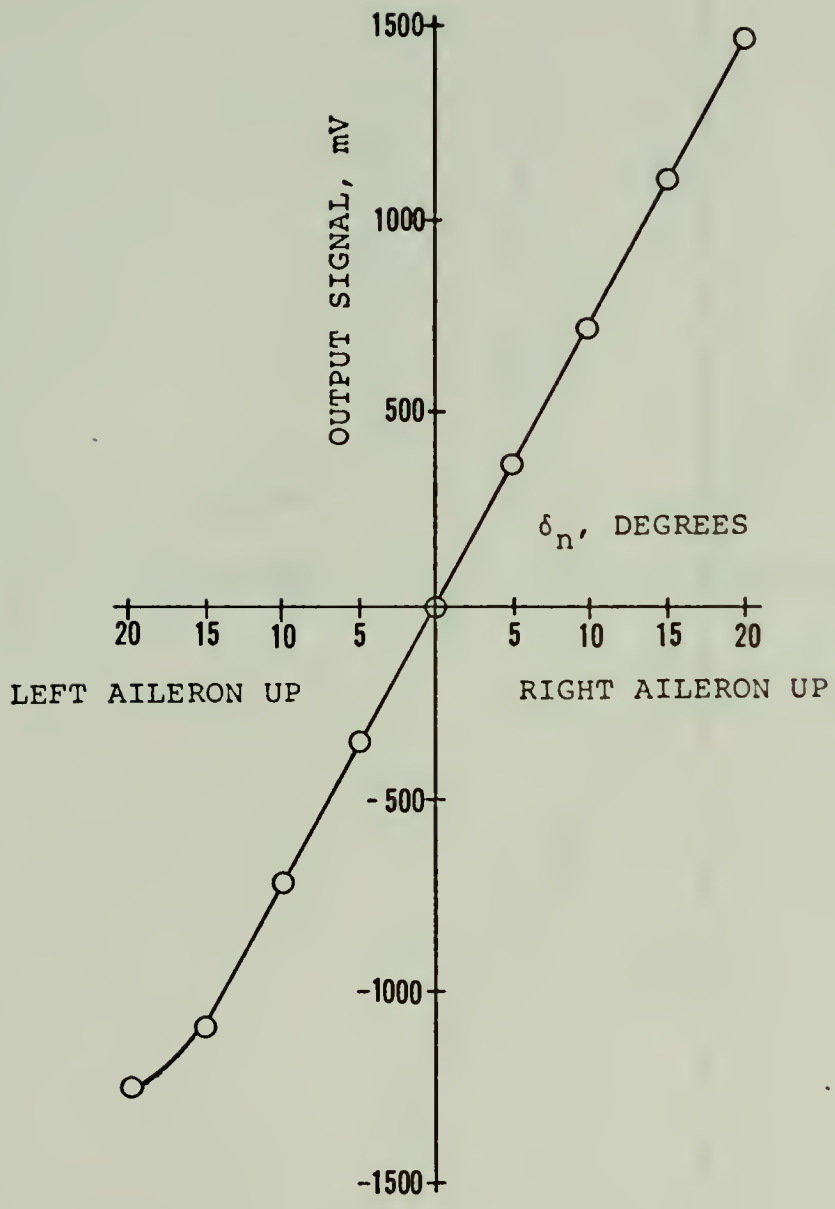

FIGURE 23. AILERON POSITION CALIBRATION CURVE

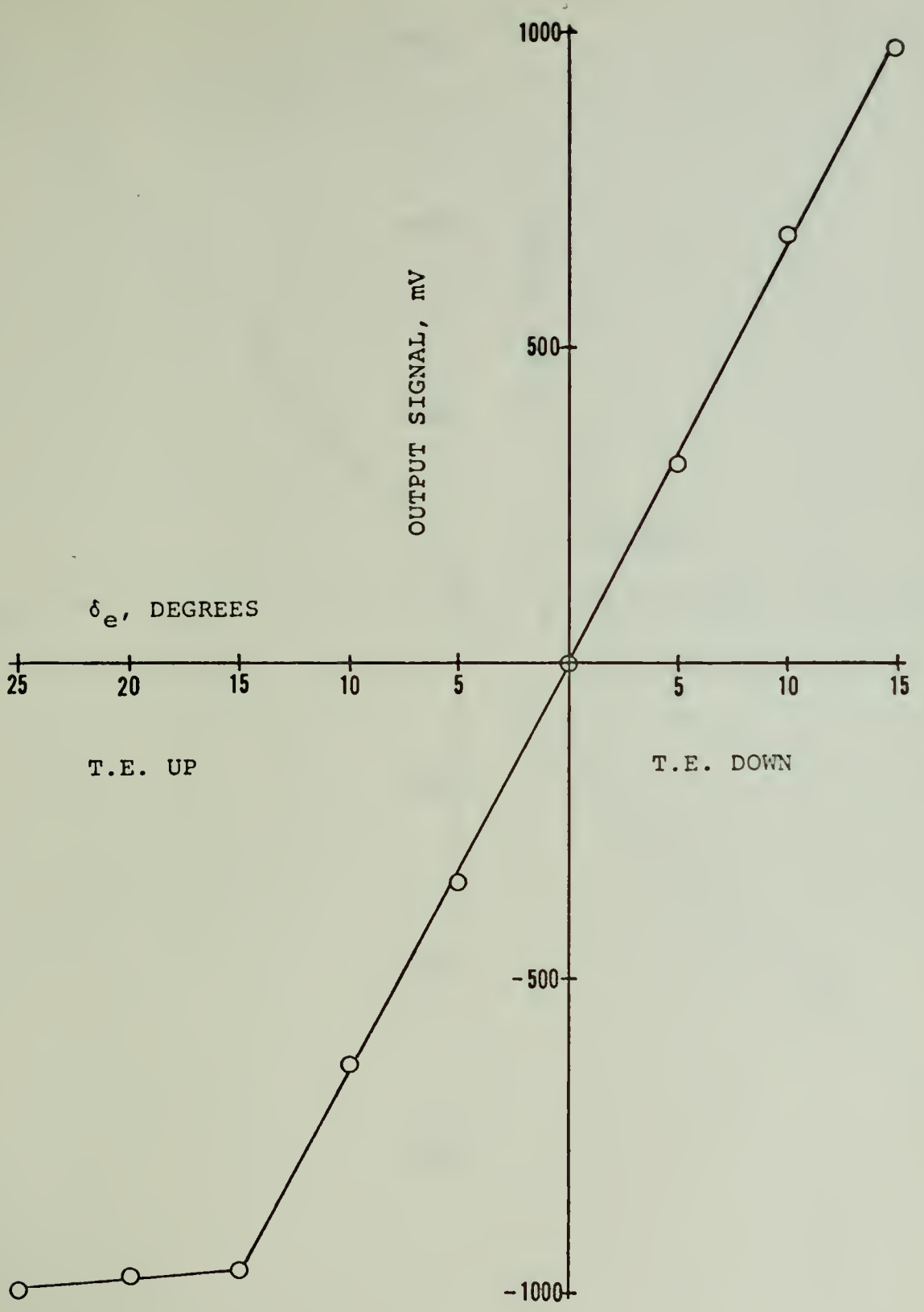

FIGURE 24. ELEVATOR POSITION CALIBRATION CURVE

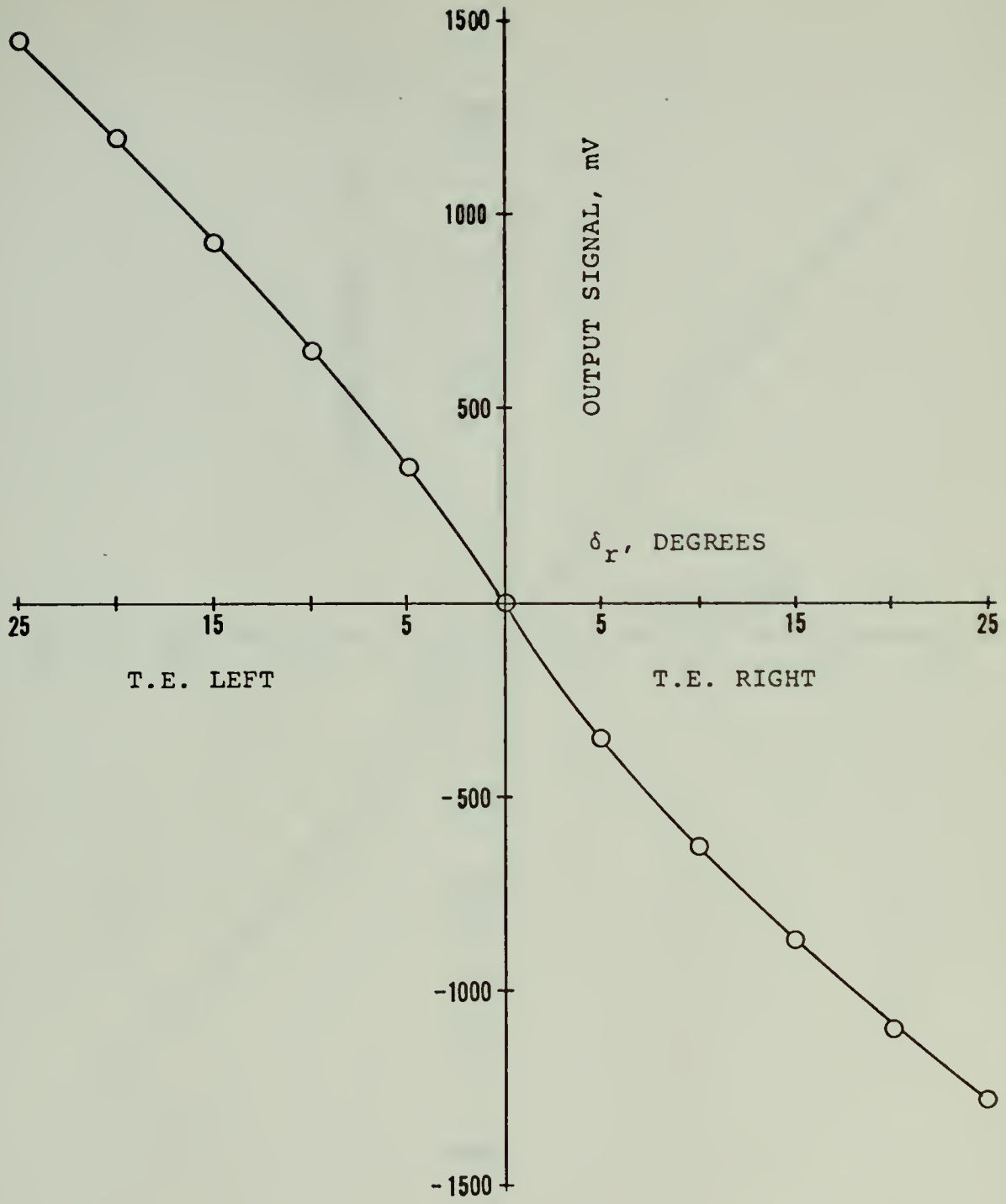

FIGURE 25. RUDDER POSITION CALIBRATION CURVE

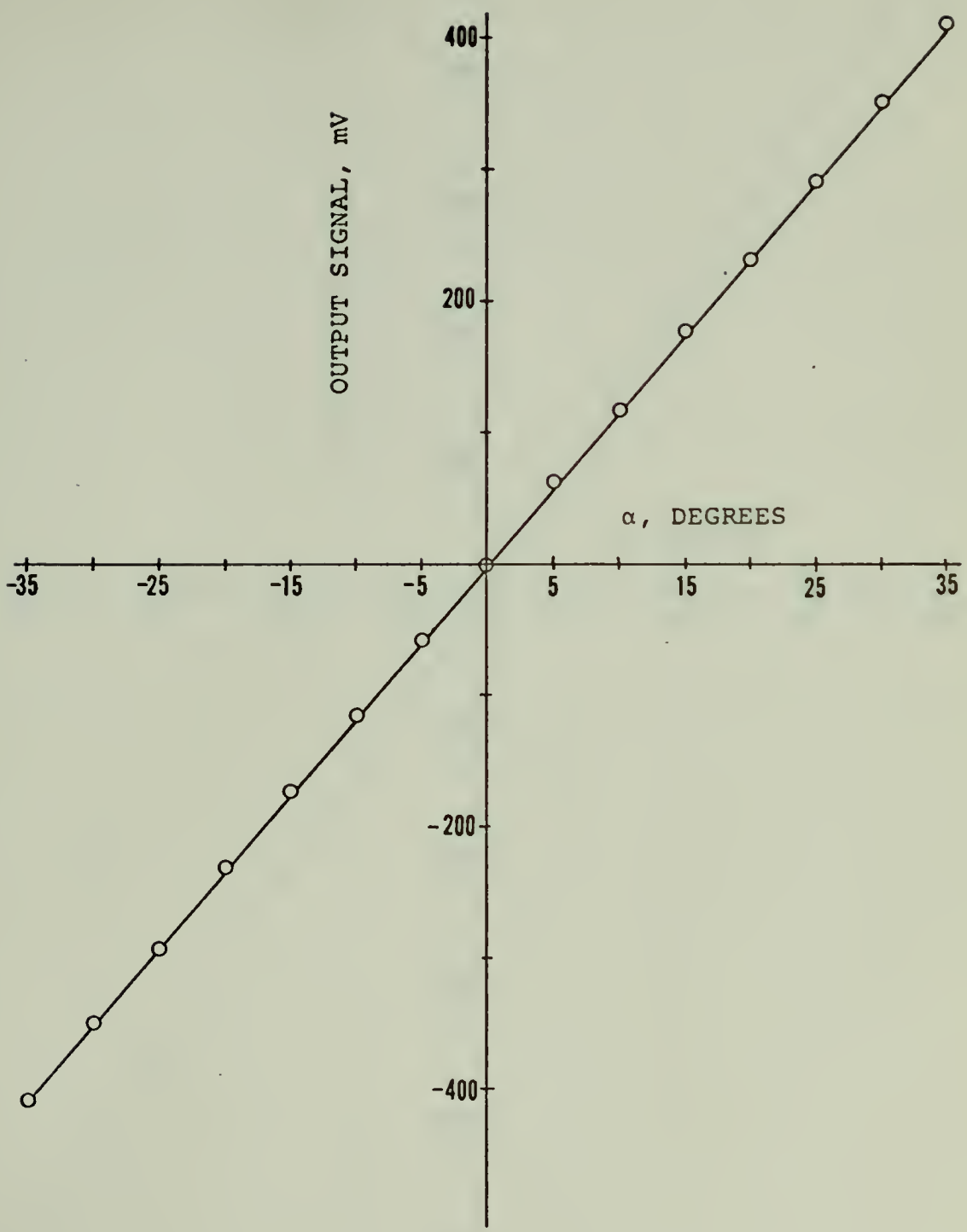

FIGURE 26. ANGLE OF ATTACK CALIBRATION CURVE

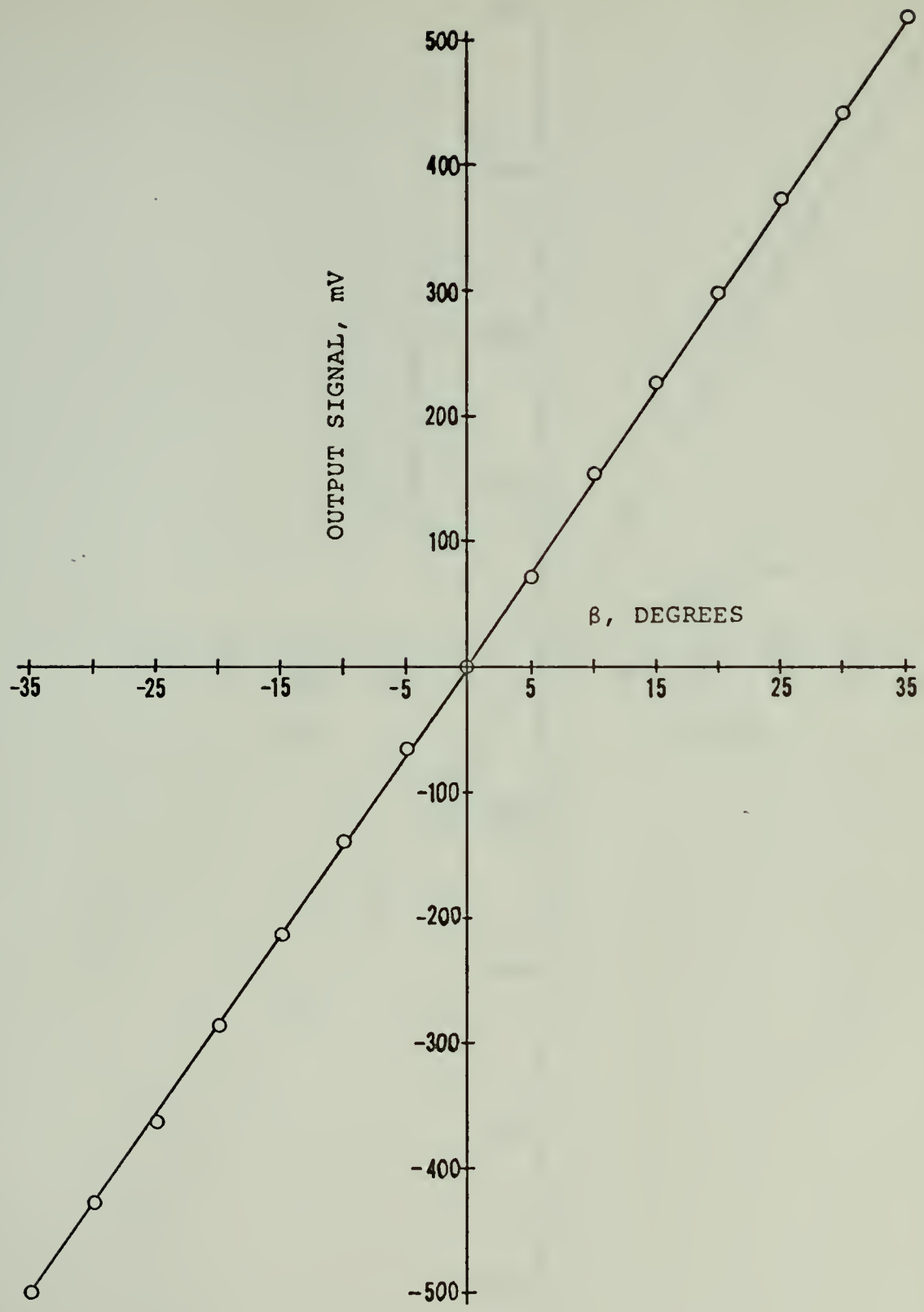

FIGURE 27. SIDESLIP CALIBRATION CURVE

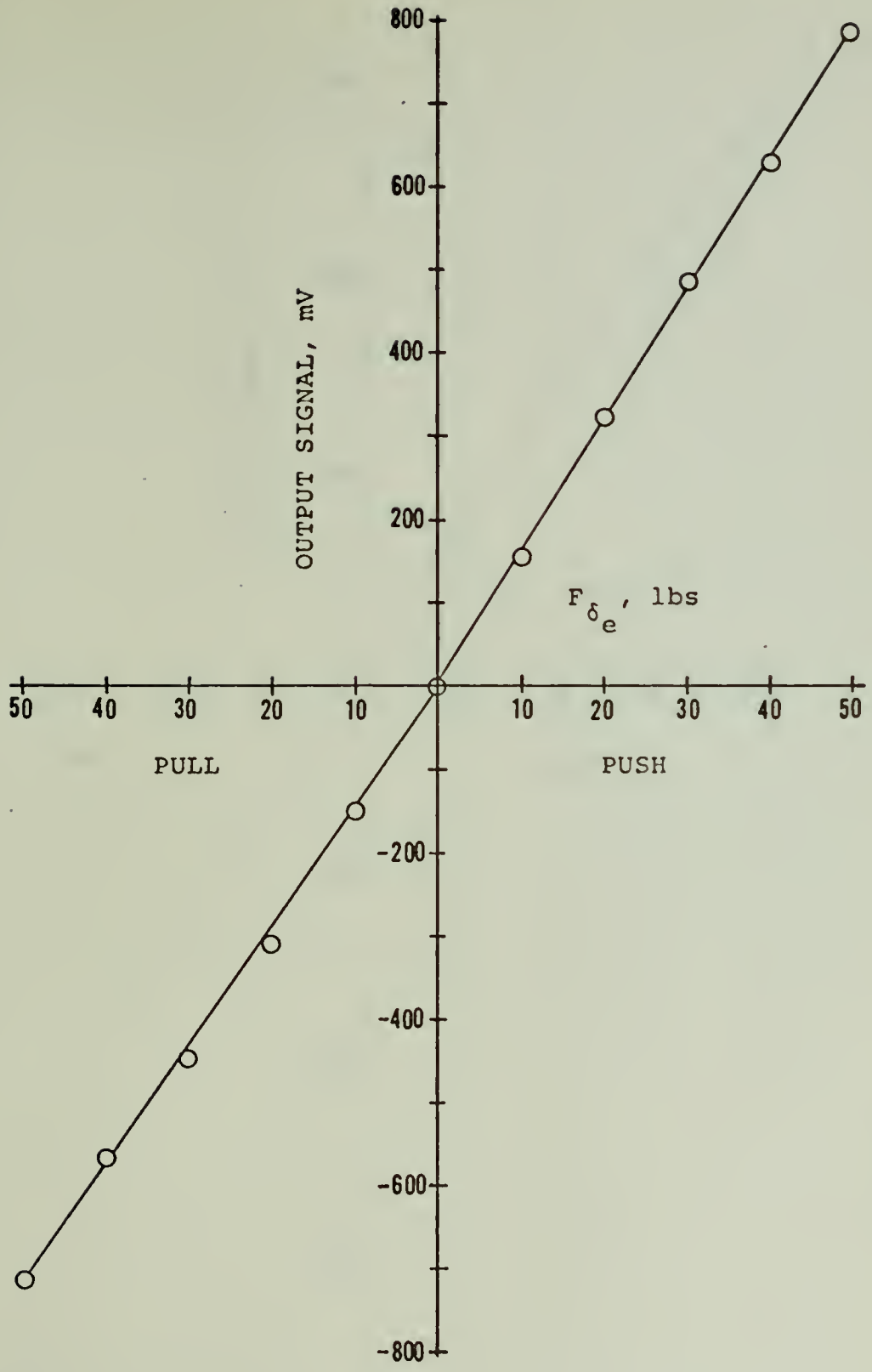

FIGURE 28. ELEVATOR FORCE CALIBRATION CURVE

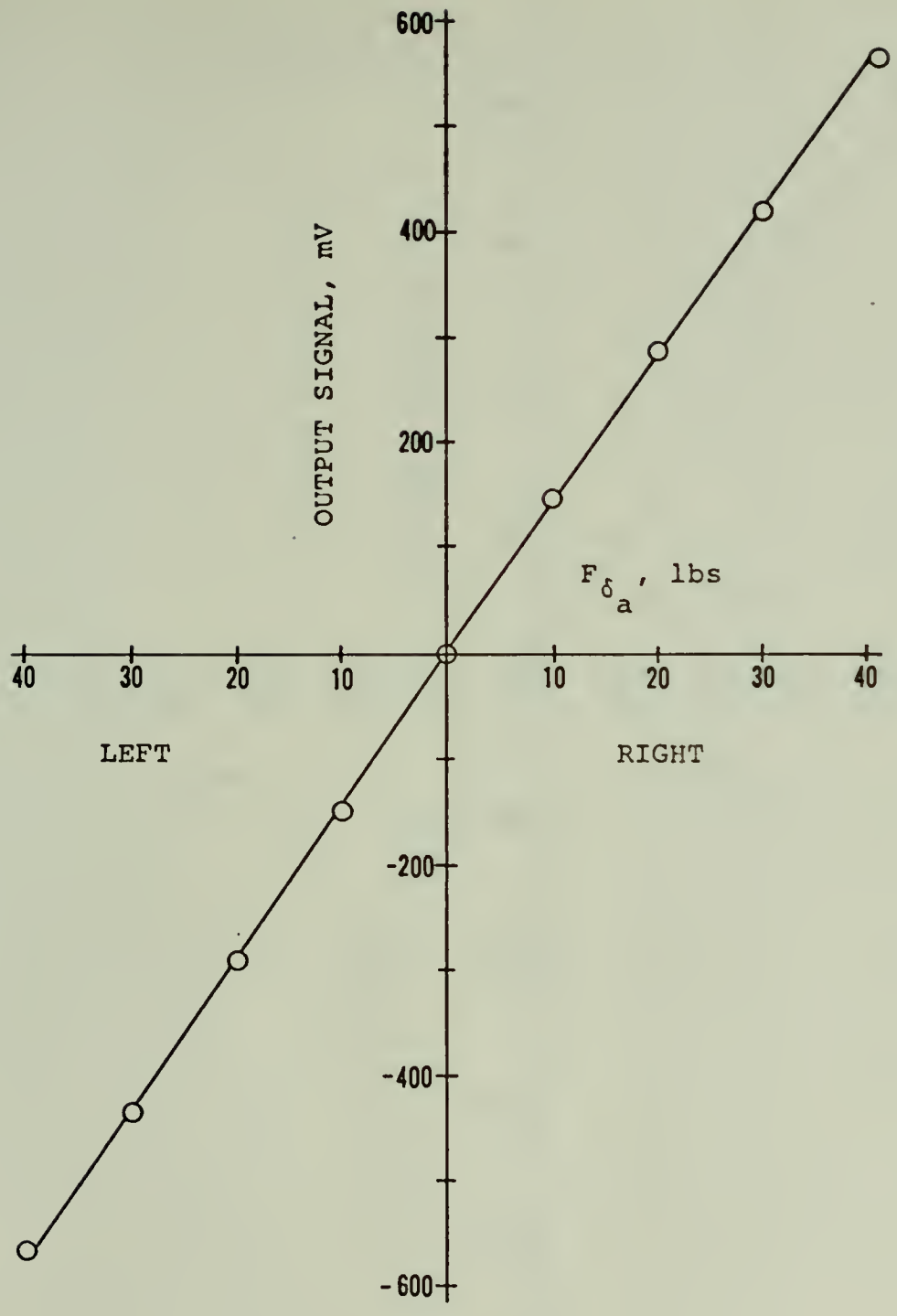

FIGURE 29. AILERON FORCE CALIBRATION CURVE

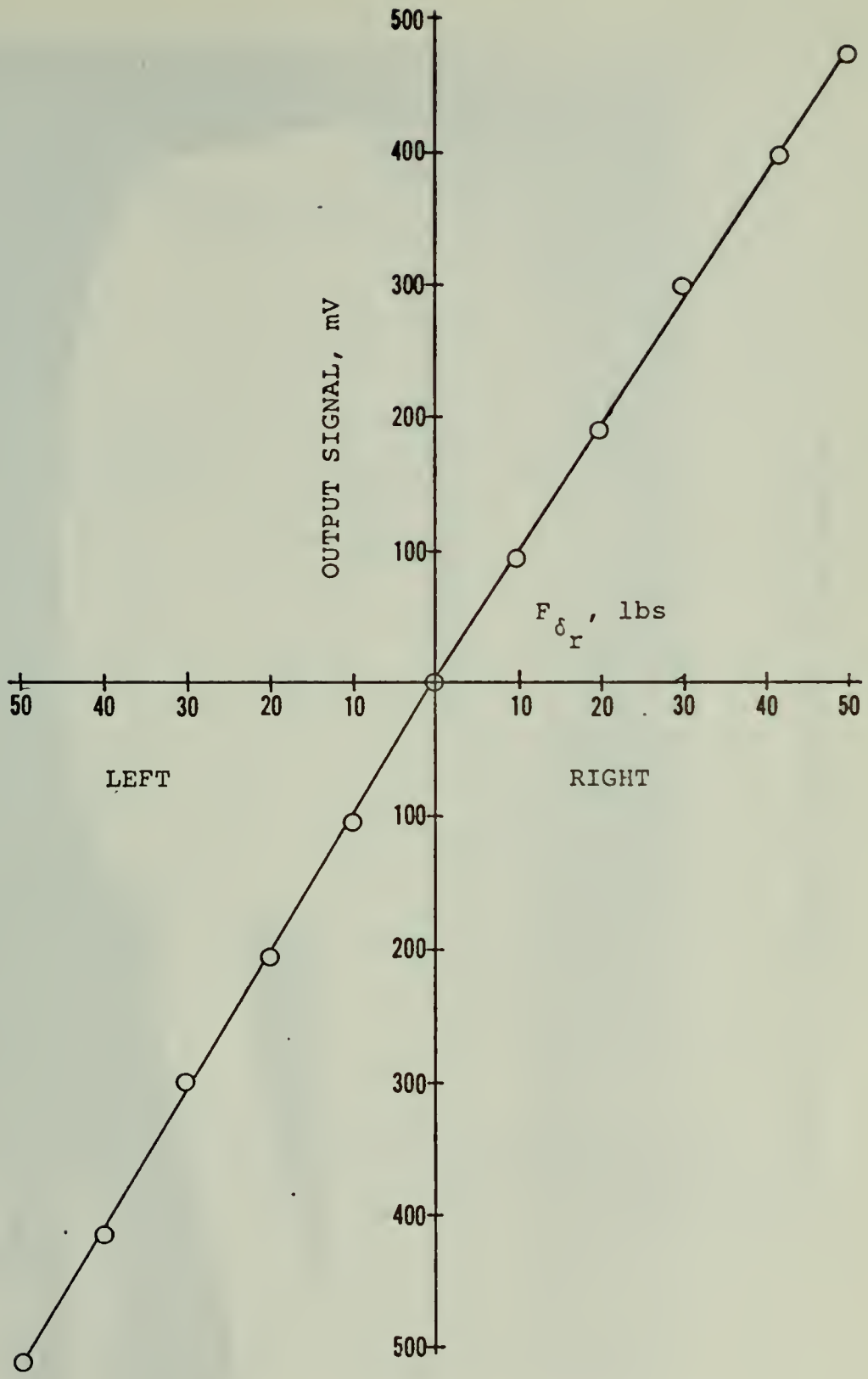

FIGURE 30. RUDDER FORCE CALIBRATION CURVE

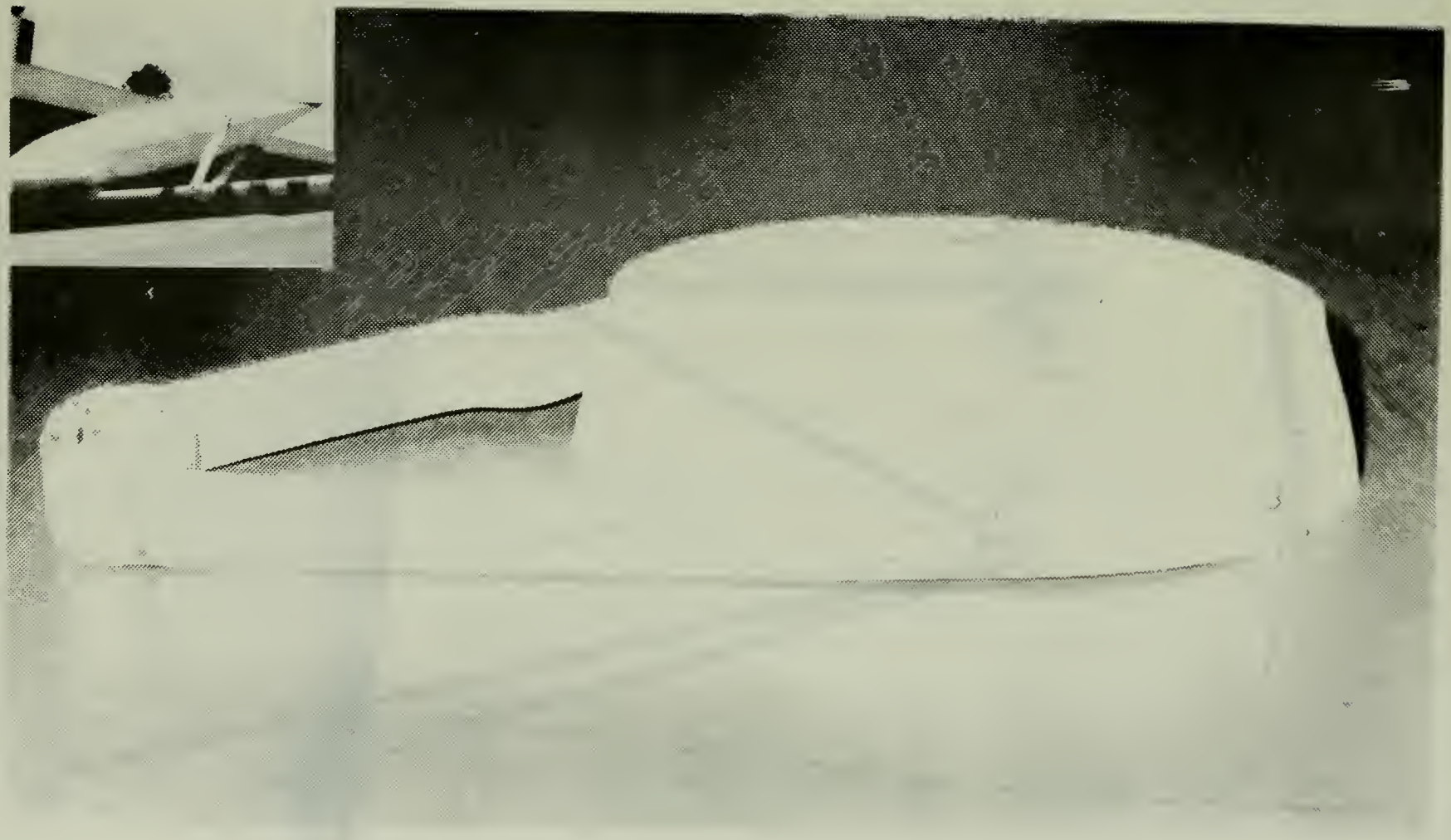

FIGURE 31. FORWARD PITOT-STATIC BOOM SUPPORT

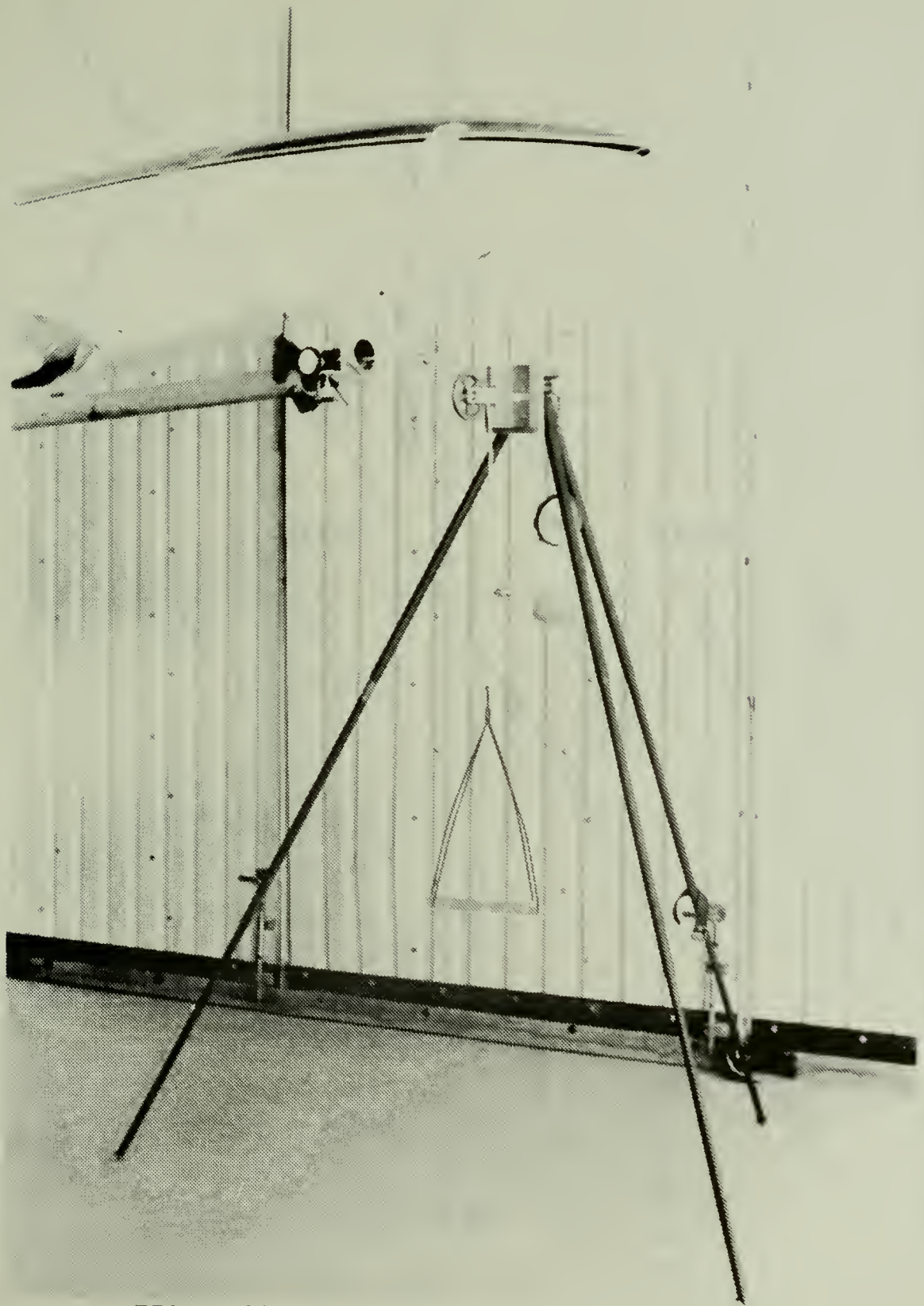

FIGURE 32. REFERENCE SET-UP FOR MEASURING BOOM SUPPORT DEFLECTION ON AIRCRAFT

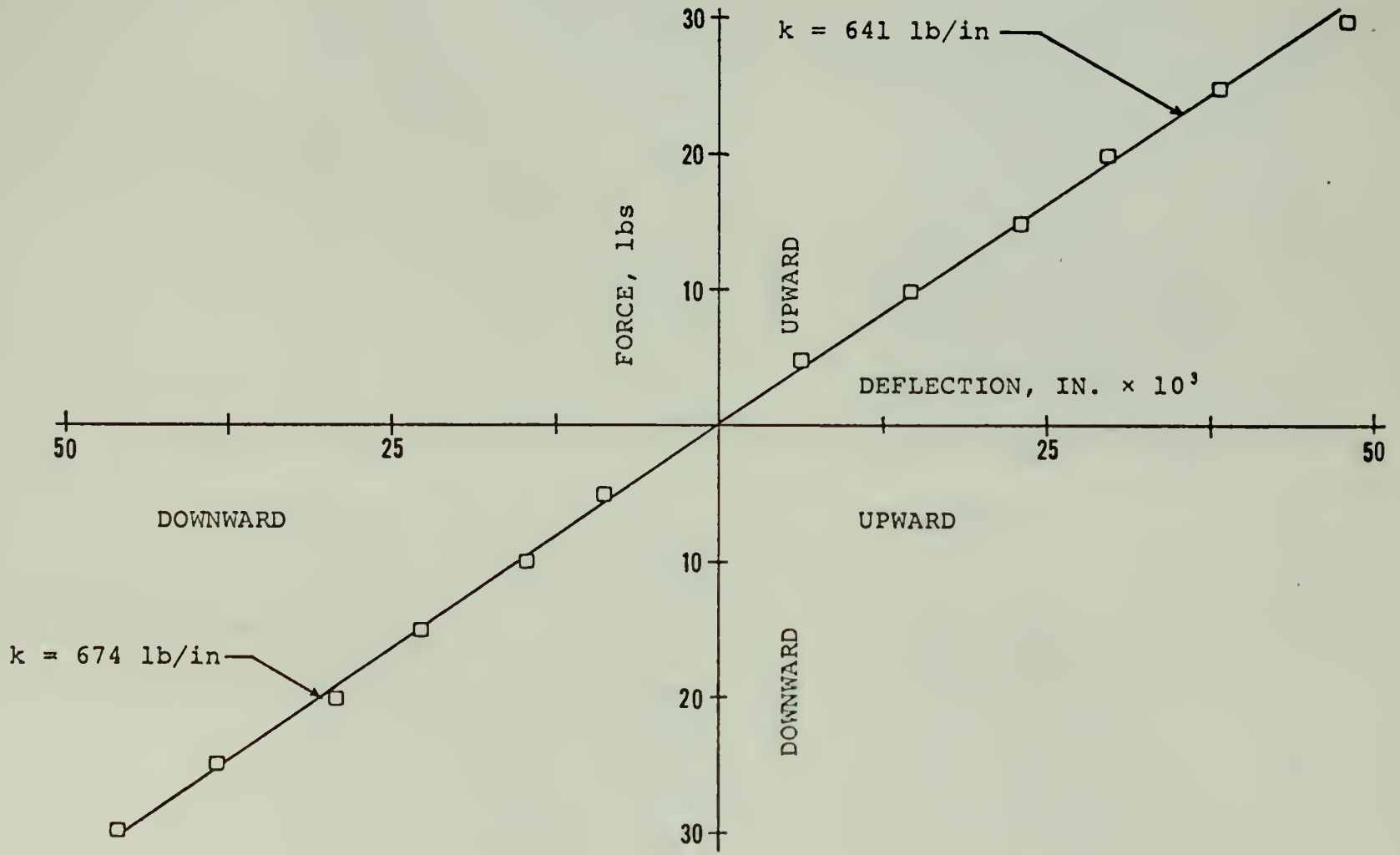

FIGURE 33. VERTICAL DEFLECTION VERSUS FORCE FOR BOOM SUPPORT ON AIRCRAFT

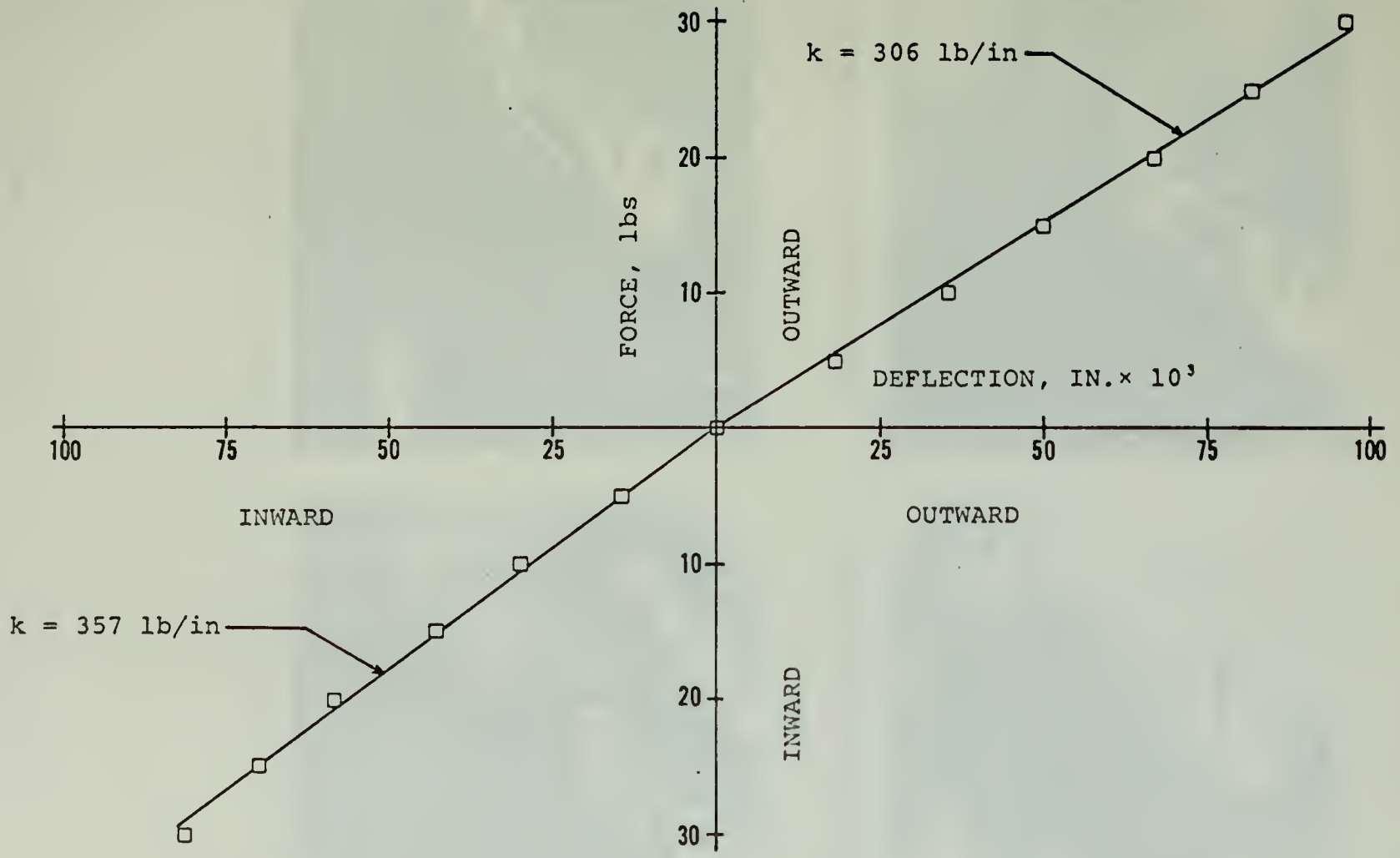

FIGURE 34. HORIZONTAL DEFLECTION VERSUS FORCE FOR BOOM SUPPORT ON AIRCRAFT

a. Loaded Vertically Upward

b. Loaded Vertically Downward

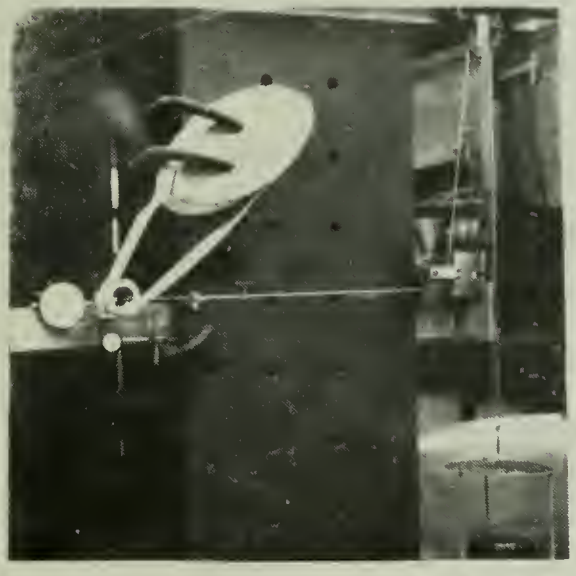

c. Loaded Horizontally Outward

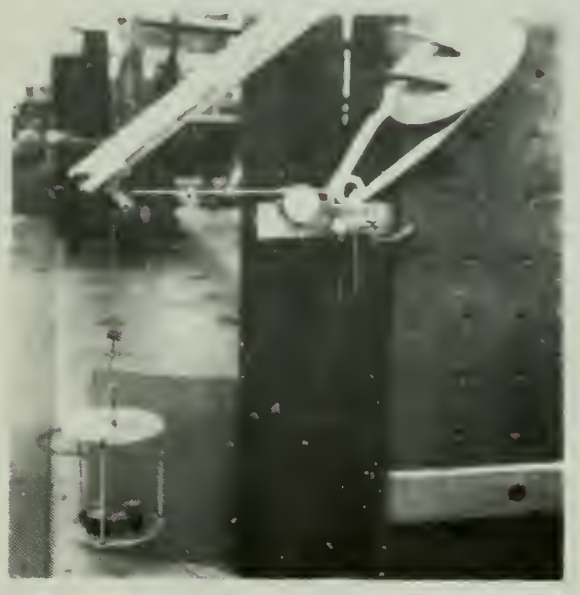

d. Loaded Horizontally Inward

FIGURE 35. REFERENCE SET-UP FOR MEASURING BOOM SUPPORT DEFLECTION IN LABORATORY

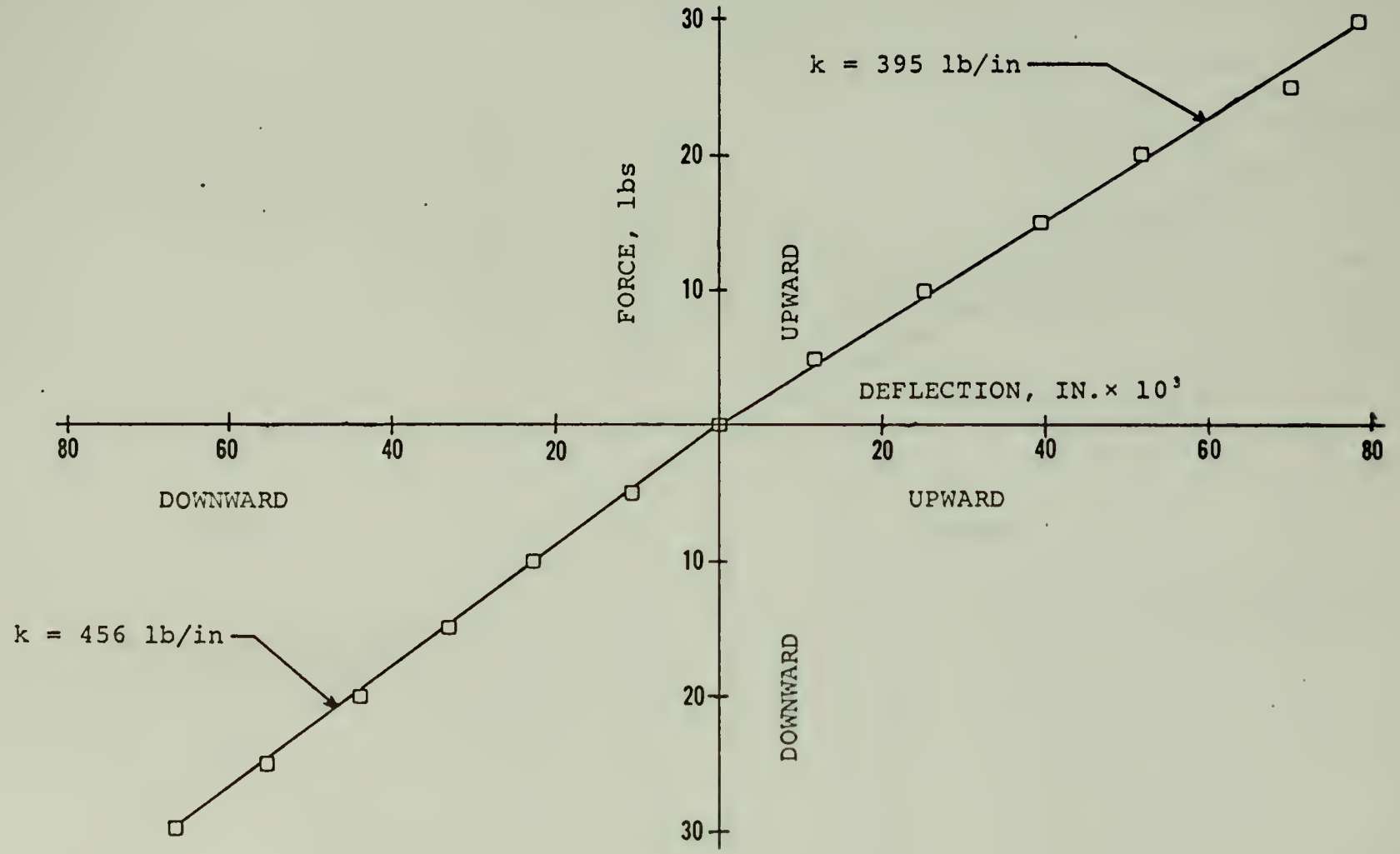

FIGURE 36. VERTICAL DEFLECTION VERSUS FORCE FOR BOOM SUPPORT IN LABORATORY

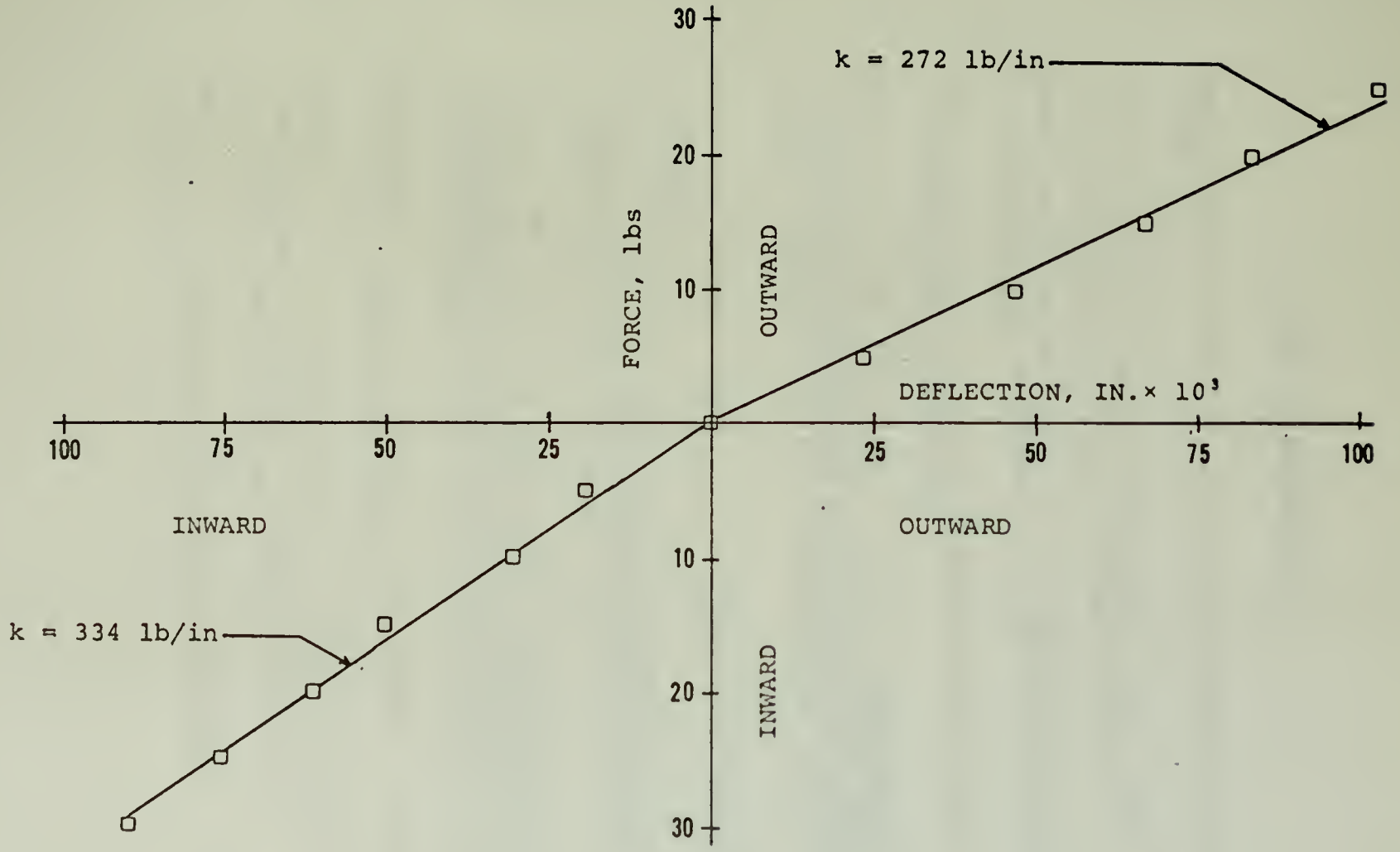

FIGURE 37. HORIZONTAL DEFLECTION VERSUS FORCE FOR BOOM SUPPORT IN LABORATORY

LIST OF REFERENCES

1. Cessna Aircraft Company, Cessna 310H Owner's Manual, 1963.

2. Cessna Aircraft Company, Cessna 310F, 310G, 310H, 310I, 310J, 310K Service Manual, December 1965.

3. Considine, D. M. and Ross, S. D., Handbook of Applied Instrumentation, McGraw-Hill, 1964.

4. Datel Systems, Inc., Datamite Series Panel Meter Specifications and Instructions.

5. Davis, G. H. and Valovich, P. J. Jr., Instrumentation of a Cessna 310H Aircraft for the Academic Investigation of Flying Qualities and Performance Characteristics, M.S. Thesis, Naval Postgraduate School, June 1973.

6. Harris, C. M. and Crede, C. E., Shock and Vibration Handbook, v. 2, McGraw-Hill, 1961.

7. N.A.S.A. TN D-3726, An Evaluation of the Handling Qualities of Seven General-Aviation Aircraft, by M. R. Barber, and others, November 1966.

8. N.A.S.A. TN D-6238, A Wind-Tunnel Investigation of Static Longitudinal and Lateral Characteristics of a Full-Scale Mockup of a Light Twin-Engine Airplane, by M. P. Fink and others, April 1971.

9. Schlichting, Hermann, Boundary Layer Theory, 4th ed., p. 27-31, McGraw-Hill, 1960.

10. Schmidt, L. V., "Measurements of Fluctuating Air Loads on a Circular Cylinder," Journal of Aircraft, v. 2, p. 49-55, January-February 1965.

11. Tong, K. N., Theory of Mechanical Vibrations, p. 279-287, John Wiley and Sons, Inc., 1960.

INITIAL DISTRIBUTION LIST

		No. Copies
1.	Defense Documentation Center Cameron Station Alexandria, Virginia 22314	2
2.	Library, Code 0212 Naval Postgraduate School Monterey, California 93940	2
3.	Chairman, Department of Aeronautics, Code 57 Naval Postgraduate School Monterey, California 93940	1
4.	Associate Professor D. M. Layton, Code 57Ln Department of Aeronautics Naval Postgraduate School Monterey, California 93940	5
5.	LT W. T. Broadhurst, USN 104 Summit Drive Brooksville, Florida 33512	1

SECURITY CLASSIFICATION OF THIS PAGE (When Data Entered)

REPORT DOCUMENTATION PAGE		READ INSTRUCTIONS BEFORE COMPLETING FORM
1. REPORT NUMBER	2. GOVT ACCESSION NO.	3. RECIPIENT'S CATALOG NUMBER
4. TITLE (and Subtitle) Installation and Validation of an Airborne Data Acquisition System Aboard a Cessna 310H for Use as a Flying Laboratory		5. TYPE OF REPORT & PERIOD COVERED Master's Thesis March 1974 6. PERFORMING ORG. REPORT NUMBER
7. AUTHOR(s) William Thomas Broadhurst		8. CONTRACT OR GRANT NUMBER(s)
9. PERFORMING ORGANIZATION NAME AND ADDRESS Naval Postgraduate School Monterey, California 93940		10. PROGRAM ELEMENT, PROJECT, TASK AREA & WORK UNIT NUMBERS
11. CONTROLLING OFFICE NAME AND ADDRESS Naval Postgraduate School Monterey, California 93940		12. REPORT DATE March 1974 13. NUMBER OF PAGES 112
14. MONITORING AGENCY NAME & ADDRESS(if different from Controlling Office) Naval Postgraduate School Monterey, California 93940		15. SECURITY CLASS. (of this report) Unclassified 15a. DECLASSIFICATION/DOWNGRADING SCHEDULE

16. DISTRIBUTION STATEMENT (of this Report)

Approved for public release; distribution unlimited.

17. DISTRIBUTION STATEMENT (of the abstract entered in Block 20, if different from Report)

18. SUPPLEMENTARY NOTES

19. KEY WORDS (Continue on reverse side if necessary and identify by block number)

Cessna 310, Data Acquisition, Pitot-Static Boom, Flight Laboratory, Vibration, Damping, Flight Controls

20. ABSTRACT (Continue on reverse side if necessary and identify by block number)

Installation and evaluation of a proposed airborne data acquisition system was accomplished for use aboard the Aeronautical Engineering Department's Cessna 310H. This flying laboratory was obtained for use with the two-course series in flight evaluation techniques to enable students to employ actual flight test methods and to gain an insight into the problems and limitations of flight testing. Static and

DD FORM 1 JAN 73 1473 EDITION OF 1 NOV 65 IS OBSOLETE
S/N 0102-014-6601 |
(Page 1)

SECURITY CLASSIFICATION OF THIS PAGE (When Data Entered)

Block 20 - ABSTRACT (Cont.)

dynamic analyses were performed on the aircraft's pitot-static boom, and a method was found to dampen vibration of the boom in flight. System calibration procedures were formulated, and the system was tested throughout the flight envelope of the aircraft. The system was found to provide satisfactory data for classroom work and will certainly improve as additional sensors are added.

Thesis
B80923
c.1

152097

Broadhurst
Installation and validation of an airborne data acquisition system aboard a Cessna 310H for use as a flying laboratory.